Draft version 0.2

CEPC NOTE

CEPC_DET_2021_001

December 25, 2020

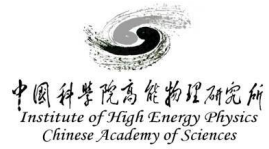

Optimization studies for the CEPC Vertex Detector

Hao Zeng

Abstract

After the CEPC Conceptual Design Report was released, the optimization of detectors is very important for the proposal of the Technical Design Report. A vertex detector prototype will be built around 2022. This note focuses on the optimization of the vertex detector based on full silicon outer tracker and including mechanics structure. A preliminary optimal vertex layout including 3 double disks and 3 same length barrel is obtained. Three new disk arrangements considering air cooling are studied. The impact of different beam pipe radius and different beam pipe material budget on vertex impact parameter resolution is investigated. The study is based on a fast silicon tracker simulation tool tkLayout.

E-mail address: zenghao@ihep.ac.cn

Contents

1 Introduction and physics requirements

The identification efficiency of heavy flavor quarks is essentially important for the CEPC physics program, hence the requirement for the CEPC vertex detector is high spatial resolution but very low material budget. In the CDR, vertex detector is mainly based on the same layout of ILD detector with several special consideration on the sensor specification. In this very ideal concept design, the detector is simplified to several material layer which do not consider real mechanical structure and electronics. In addition, the CDR vertex design do not provide a solution for air cooling which is indispensable to save vertex detector material budget. In order to build a real vertex detector, we take into account many engineering details of the vertex detector in this note.

In the CEPC Conceptual Design Report, the ILD vertex layout, which contains three double layers in the barrel and two single disks in the endcap, is directly used without any documented studies on vertex layout for CEPC. Considering transverse impact parameter resolution as criteria, we get a very ideal vertex layout which do not consider air cooling after we studied many different vertex layouts. Because of the excellent performance of tkLayout in silicon tracker fast simulation, all outer trackers used in our simulation are full silicon outer trackers which come from CDR and possibly replace current TPC design. Meanwhile, we also make a comparison of transverse impact parameter resolution for different full silicon trackers of CDR.

The impact of beam pipe radius and material on the vertex impact parameter resolution is also studied. The first layer of our vertex detector is directly mounted on the beam pipe, so the beam pipe radius will affect the radius of vertex first layer. Also beam pipe material will affect the total material budget of vertex region and therefor affect the vertex physics performance.

2 CEPC Tracker design

2.1 CDR vertex layout

The baseline layout of the CEPC vertex detector consists of six concentric cylindrical layers of high spatial resolution silicon pixel sensors located between 16 and 60 mm in radii from the beam line (see Figure 1), providing six precise space-points for charged particles traversing the detector [1]. The main mechanical structure is called a ladder. Each ladder supports sensors on both sides; thus, there are three sets of ladders for the vertex detector. The material budget of each detector layer amounts to $\sim 0.15\%$ X_0, including their corresponding supporting material. The layout configuration and sensor single-point resolution are listed in Table 1.

	R (mm)	$\lvert z\rvert$ (mm)	$\lvert\cos\theta\rvert$	$\sigma(\mu m)$
Layer 1	16	62.5	0.97	2.8
Layer 2	18	62.5	0.96	6
Layer 3	37	125.0	0.96	4
Layer 4	39	125.0	0.95	4
Layer 5	58	125.0	0.91	4
Layer 6	60	125.0	0.90	4

Table 1: The baseline design parameters of CEPC vertex detector including position and single-point resolution. The values of single-point resolution for layer 1 and layer 2 consider a double-sided ladder concept based on a high resolution sensor on one side, and a faster sensor on the other side to provide necessary time-stamp for tracking.

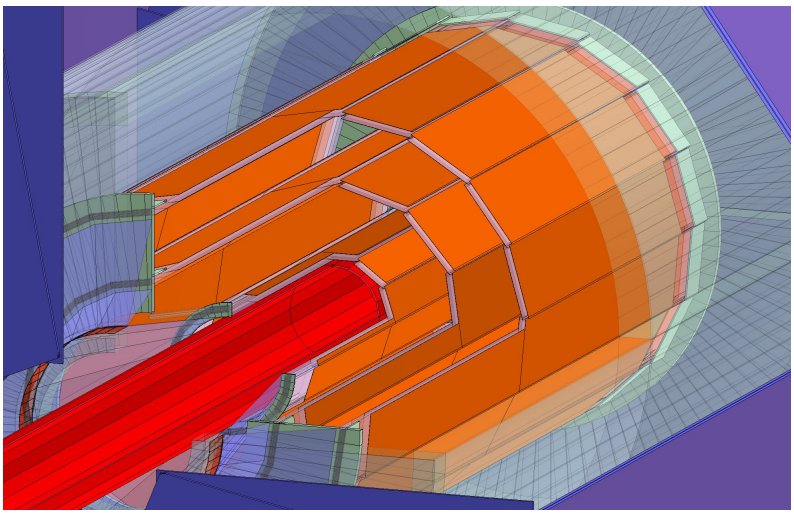

Figure 1: Schematic view of pixel detector. Two layers of silicon pixel sensors are mounted on both sides of each of three ladders to provide six space points. Only the silicon sensor sensitive region (in orange) is depicted. The vertex detector surrounds the beam pipe (red).

2.2 CDR full silicon tracker

In CEPC CDR [1], two layouts of full silicon tracker, called FST and FST2, have been investigated. A full silicon tracker consists of VXD, EIT, SOT and EOT. SOT (Silicon Outer Tracker) is the outermost tracker of the full silicon tracker, usually consists of strip layer. EOT (Endcap Outer Tracker) is the strip disk placed at either side of the SOT. VXD represents the barrel region of the vertex detector, while EIT (Endcap Inner Tracker) is the pixel disk placed at either side of IP inside the EOT. The geometric parameters of two full silicon tracker concept are given in Table 2 and Table 3.

FST has a SOT with six double-strip layers and an EOT with five double-strip disks, whose VXD has two single pixel layers inside and two double pixel layers outside. The FST can provide 12 precise space point measurements (6 from the vertex detector and 6 from the silicon trackers) in the central barrel region, and at least 7 points in front endcap region. Differing from FST, FST2 has a SOT with five single-strip layers and an EOT with four double-strip disks, five single pixel layer for VXD near IP and seven single pixel disks placed at different position for EIT. FST2 only can provide 10 space measurement points in the very central region. FST and FST2 layouts are shown in Figure 2.

3 Tool(s) and validation

3.1 Simulation tool

All the simulation results in this note are based on fast simulation tool tkLayout, which is developed by CMS collaboration for HL-LHC CMS tracker R&D and FCC-hh tracker conceptual design. tkLayout only takes time in the order of minutes to automatically compute the module coordinates and then to get physics performance result which is very close to full simulation result. In addition, its simulation contains more mechanical details and various material components than other silicon tracker fast simulation tool. You can easily obtain all simulation result on webpage after running some configuration files which are very easy to learn how to write. Though tkLayout has many advantages, it is developed for CMS tracker optimization and has many hard codes. We keep contact with tkLayout development team during our simulation study and successfully add some new functions for CEPC. For instance, adding

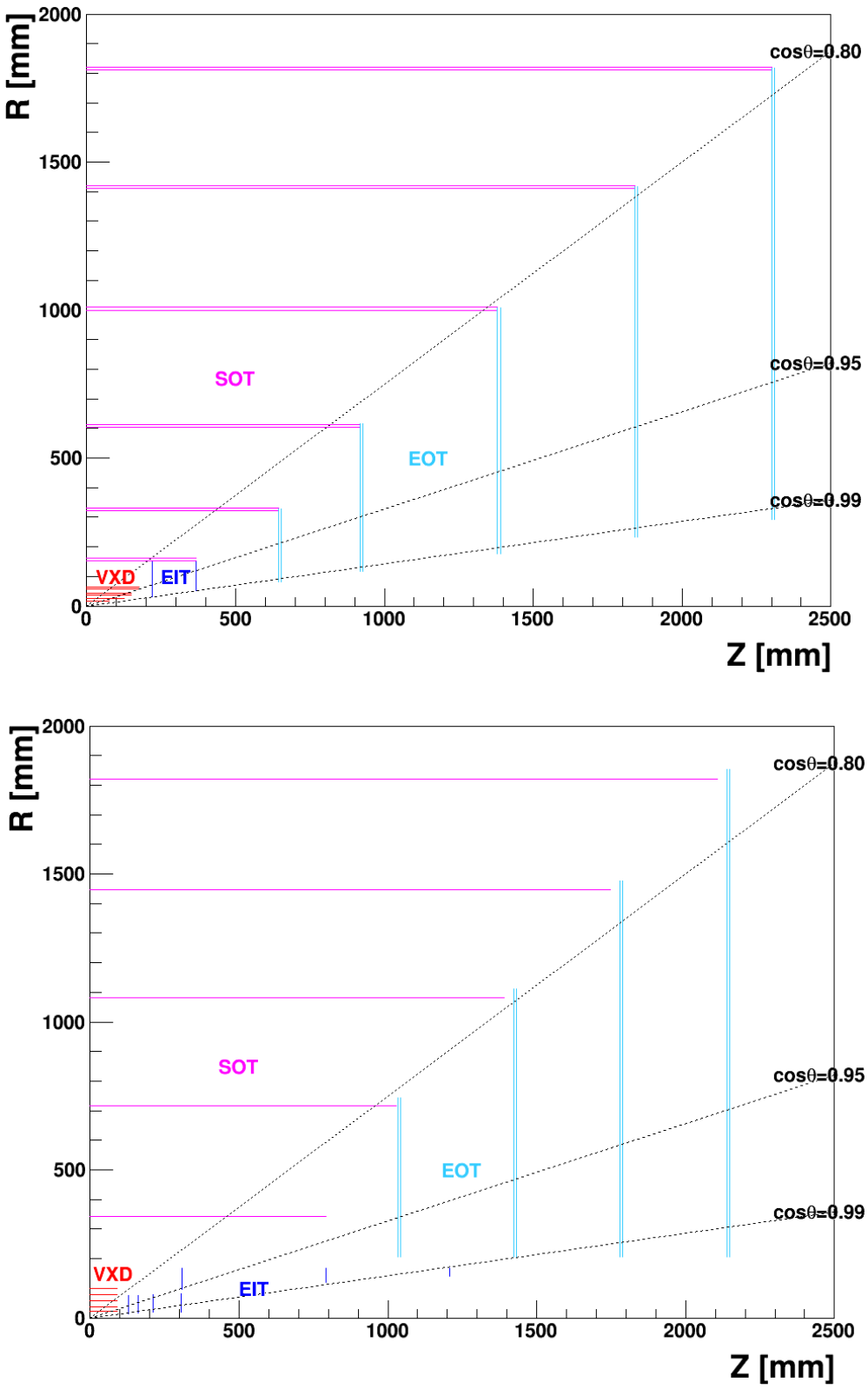

Figure 2: $R-Z$ views of the full-silicon tracker options, FST (top) and FST2 (bottom). In the FST layout, the full strip detector (SOT and EOT) is composed of double silicon strip layers. In the FST2 layout, the SOT consists of single layers, while the EOT consists of double-strip layers.

	FST			FST2		
VXD	R (m)		$\pm z$ (m)	R (m)		$\pm z$ (m)
Layer 1	0.016		0.078	0.022		0.091
Layer 2	0.025		0.125	0.038		0.091
Layer 3	0.037		0.150	0.058		0.091
Layer 4	0.038		0.150	0.079		0.091
Layer 5	0.058		0.175	0.100		0.091
Layer 6	0.059		0.175			
EIT	R_{in} (m)	R_{out} (m)	$\pm z$ (m)	R_{in} (m)	R_{out} (m)	$\pm z$ (m)
Disk 1	0.030	0.151	0.221	0.014	0.076	0.129
Disk 2	0.051	0.151	0.368	0.016	0.077	0.162
Disk 3				0.018	0.079	0.212
Disk 4				0.020	0.082	0.306
Disk 5				0.097	0.167	0.308
Disk 6				0.121	0.167	0.792
Disk 7				0.142	0.167	1.207

Table 2: Geometric parameters of the silicon pixel detectors of the FST and FST2. The vertex detector has six layers for the FST option and five layers for the FST2 option. The EIT has two disks in the FST case, and seven disks in the FST2 case.

	FST				FST2			
SOT	R (m)		$\pm z$ (m)	Type	R (m)		$\pm z$ (m)	Type
Layer 1	0.153		0.368	D	0.344		0.793	S
Layer 2	0.321		0.644	D	0.718		1.029	S
Layer 3	0.603		0.920	D	1.082		1.391	S
Layer 4	1.000		1.380	D	1.446		1.746	S
Layer 5	1.410		1.840	D	1.820		2.107	S
Layer 6	1.811		2.300	D				
EOT	R_{in} (m)	R_{out} (m)	$\pm z$ (m)	Type	R_{in} (m)	R_{out} (m)	$\pm z$ (m)	Type
Disk 1	0.082	0.321	0.644	D	0.207	0.744	1.034	D
Disk 2	0.117	0.610	0.920	D	0.207	1.111	1.424	D
Disk 3	0.176	1.000	1.380	D	0.207	1.477	1.779	D
Disk 4	0.234	1.410	1.840	D	0.207	1.852	2.140	D
Disk 5	0.293	1.811	2.300	D				

Table 3: Geometric parameters of the silicon strip detectors of the FST and FST2. Types S and D stand for single- and double-strip layer, respectively. The FST design has six double-strip layers for the SOT and five double-strip disks for the EOT, whereas the FST2 design has five single-strip layers for the SOT and four double-strip disks for the EOT.

a new parameter skewed angle which can control the ladder rotation around z axis (see Figure 3) and changing all η description often used in hadron collider to cosθ description often used in lepton collider

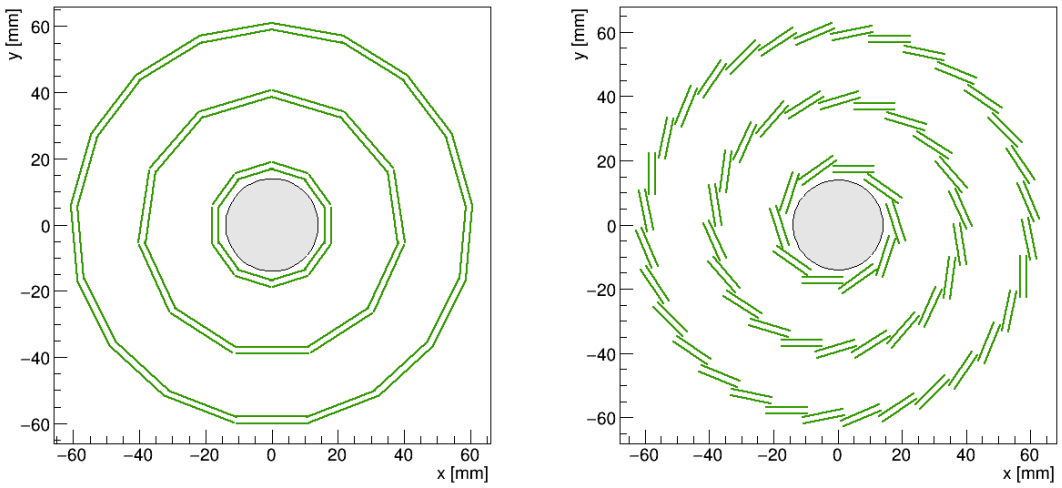

(a) CDR vertex layout

(b) prototype_v1 vertex layout

Figure 3: The comparison of CDR vertex layout and prototype_v1 vertex layout: (a)The CDR vertex layout which consists of three concentric regular polygon and (b)the prototype_v1 vertex layout whose ladders are rotated by small angle around the z axis.

(see Figure 4).

3.2 Simulation tool validation

The validation of this fast simulation tool is necessary because this is the first time we use tkLayout for CEPC vertex layout optimization. Here we choose the full silicon tracker FST and FST2 as reference to compare the CDR simulation results with the tkLayout simulation results. Figure 5 shows that the d0 resolution, as a function of Pt, is compared for different full silicon tracker, using single muon tracks with polar angle $\theta = 85°$ and $20°$. The top plot in Figure 5 is the simulation results from CDR while the bottom plot shows the simulation results using tkLayout. We can see that the resolution curves of CDR and tkLayout are the same shape and the resolution minimum of them are very close.

4 New design and optimizations

The vertex baseline in this note is the CDR vertex and outer tracker is also from CDR full silicon tracker. The prototype_v1 is the geometry that uses the same radius parameters as CDR vertex but rotating the ladder a small skewed angle around z axis for engineering requirement, which is the method we build vertex barrel in this note (see in Figure 3).

In order to study the performance of whole tracking system, in addition to vertex tracker, an outer tracker is also needed. In this note, we choose the outer tracker of FST as the fixed outer tracker for vertex optimization because we find that the outer tracker of FST has better transverse impact parameter resolution due to more layers providing more measurement points. And then we study the impact of vertex size, number of layers and the radius of second layer on the vertex transverse impact parameter resolution. The result shows that the effect of these variations on vertex d0 resolution is very small, so we choose the original prototype_v1 design as better geometry considering the feasibility of mechanics installation. And then we compare the resolution of the prototype_v1 layout to the resolution of the long barrel vertex which is a vertex design without endcap and will be introduced in 4.5. We find that the

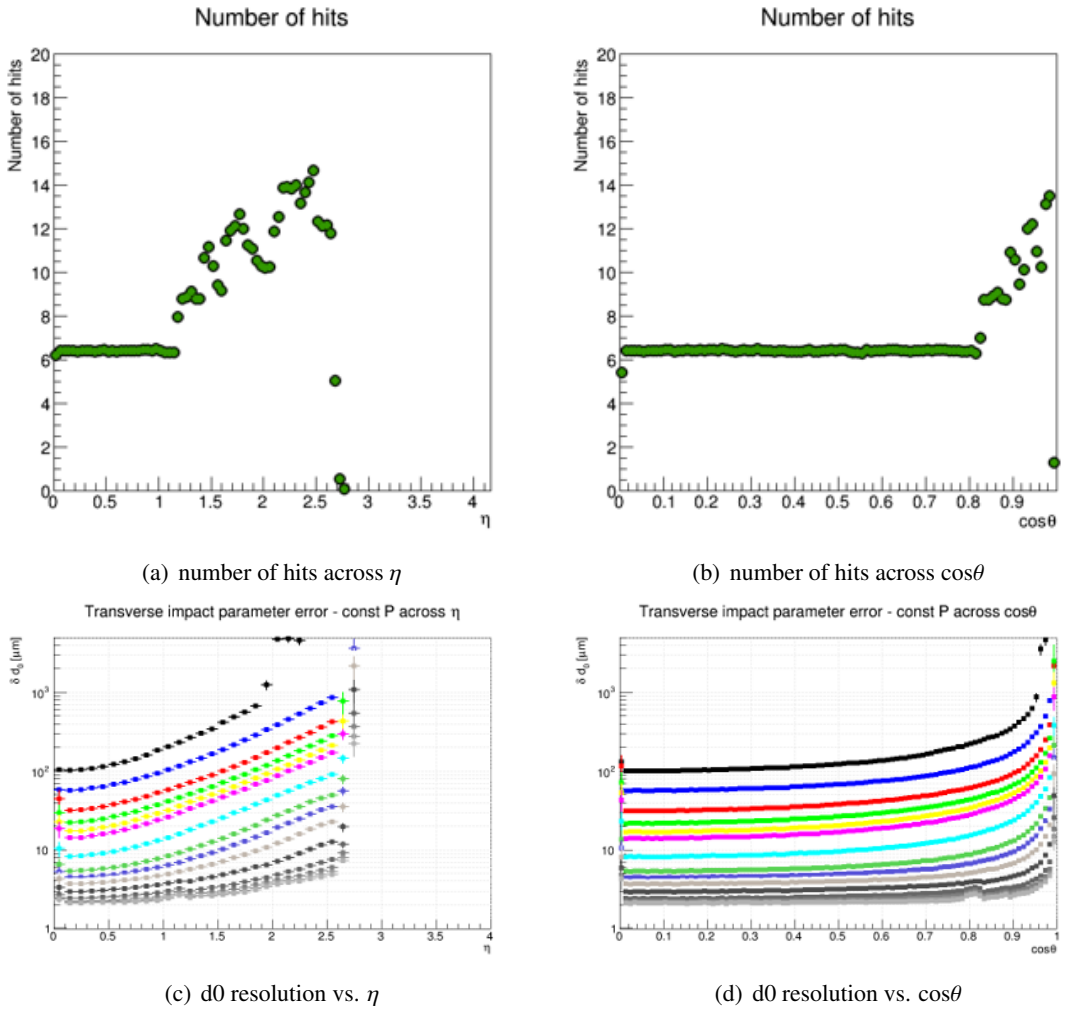

(a) number of hits across η

(b) number of hits across cosθ

(c) d0 resolution vs. η

(d) d0 resolution vs. cosθ

Figure 4: Two examples of changing η to cosθ. Left column is the original output plots of tkLayout while right column is the new output plots after changing the η to cosθ.

ideal long barrel design has better resolution than prototype_v1 design. Finally, we extend the first barrel layer of prototype_v1 and optimize the CDR vertex endcaps, and then get an optimal vertex layout which contains three same length double layer in barrel and three double disks in the endcap.

4.1 Module introduction

In tkLayout, tracker is built with modules which is the basic element of tracker like building block. Considering realistic detector, we use different types of module for different sub-tracker. For instance, we define two types of module (pixel module and strip module) in this note. Pixel module, used for single pixel layer and double pixel layer in VXD and EIT, has the size of 12.8mm × 25.6mm. Strip module has the size of 100mm × 92mm, which is used for SOT and EOT of outer tracker. In addition to the geometry properties, the module has material property which can help you to estimate the detector material budget as you can add various material into the module. We have done many simulation work for the module material, you can see more details in Appendices. For a actual detector, we should not only consider the material for the module, but also the material for the mechanical structure, cable and service. In this note, we have considered the material of ladder support structure and dead material of

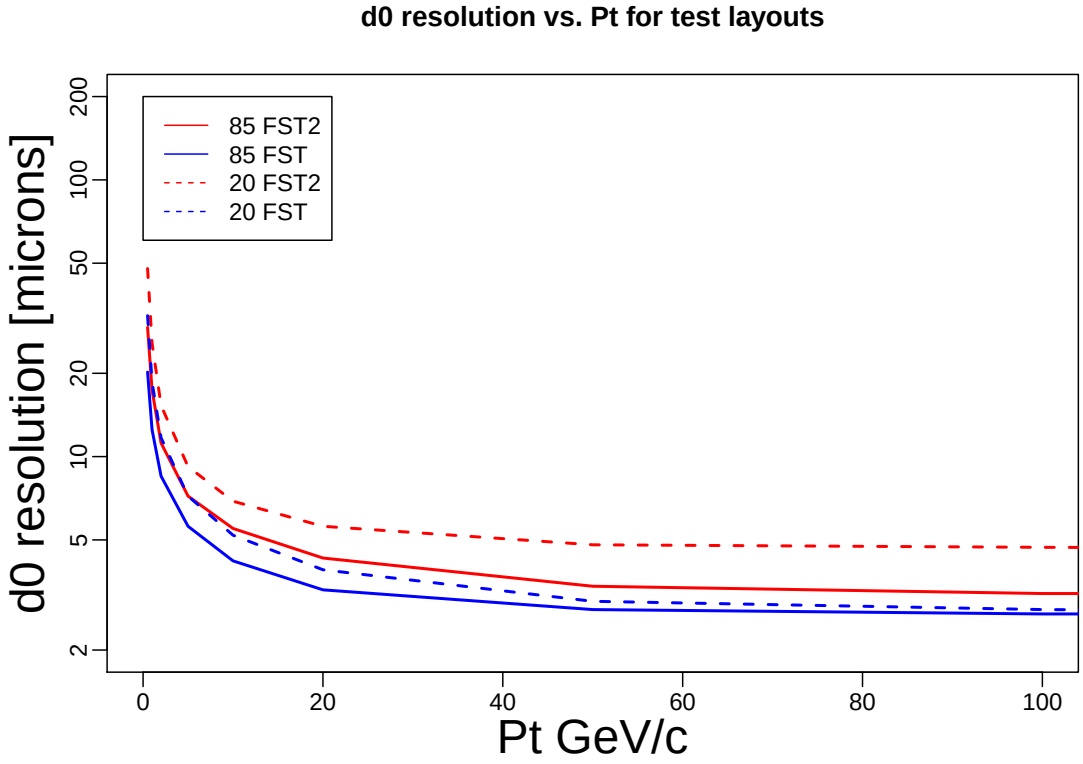

(a) d0 resolution vs. Pt from CDR

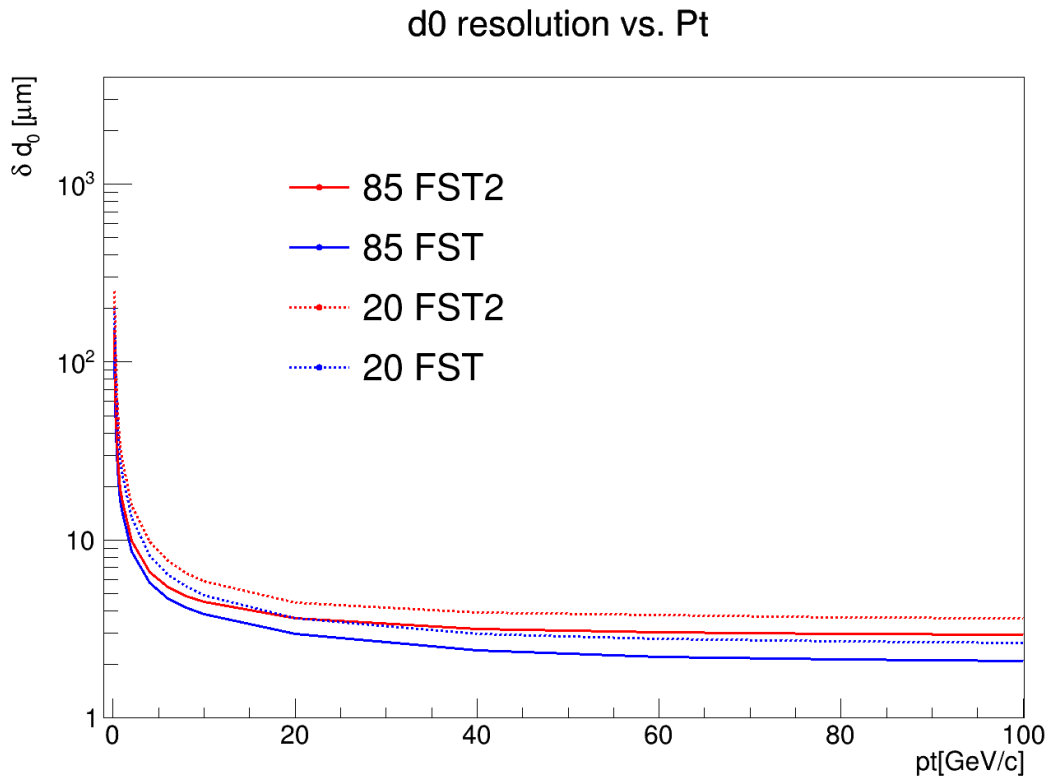

(b) d0 resolution vs. Pt from tkLayout simulation

Figure 5: Validation of tkLayout for d0 resolution: (a) d0 resolution for FST and FST2 with polar angle θ=85° and 20° from CDR simulation results; (b) d0 resolution for FST and FST2 with polar angle θ=85° and 20° from tkLayout simulation results.

module for VXD. For EIT, the material components are the same as VXD because we using the same module as VXD. While for SOT and EOT, we just directly using the double-strip module and single-strip module of CMS because we have no module level study for outer full silicon tracker. In addition, we only take into account the module material for outer tracker.

4.2 Prototype_v1 layout variations

Because the vertex layout of CEPC is directly copied from ILD vertex, there is no documented study on why we choose this vertex geometry. The first thing we want to investigate is to change the CDR vertex layout to see the performance of this variations of CDR vertex layout. Now we have a vertex layout prototype_v1 considering mechanics design, so we can directly change the prototype_v1 geometry for this CDR vertex variation study.

Firstly, we study the effect of the vertex detector size on the transverse impact parameter resolution. Here we investigate three different size of detectors: 60mm (This is the same size of prototype_v1, we take it as reference.), 80mm and 100mm. We keep the vertex detector the same as prototype_v1 with three double pixel layers and placed equidistantly when changing the size of the detector. All detector parameters are listed in Table 4 and all layouts are shown in Figure 6.

	prototype_v1	**R=80mm**	**R=100mm**
double-layer	R (mm)	R (mm)	R (mm)
Layer 1	18	18	18
Layer 2	38	49	59
Layer 3	60	80	100

Table 4: Double-layer radii for different detector size: r=60mm (prototype_v1), r=80mm and r=100mm

Because we only change the layer radii of barrel region, we only care about the d0 resolution in very central region. The d0 resolution, as a function of momentum, is compared for different detector size using single muon tracks with polar angle $\theta = 87°$ and $60°$ in Figure 7. We can see that the d0 resolution is no big difference for different detector size at very low momentum like 0.1GeV to 1GeV, while the d0 resolution is different at higher momentum like 1GeV to 100GeV. For instance, bigger vertex detector has better resolution with momentum from 1GeV to 10GeV and smaller vertex detector has better resolution (because the first measurement point is closer to the beam pipe).

Secondly, we study the effect of the number of layer on the transverse impact parameter resolution. We fix the size of the detector at 60mm and then change the number of double layers to 2, 3 and 4 but still keeping every layer placed equidistantly. All detector parameters are listed in Table 5 and all layouts are shown in Figure 8.

The d0 resolution, as a function of momentum, is compared for different detector size using single muon tracks with polar angle $\theta = 87°$ and $60°$ in Figure 9. We can conclude that:

- 0.1GeV-1GeV: The effect of number of layers on d0 resolution is very small.
- 1GeV-10GeV: The vertex with less layers has better d0 resolution, which may be because material effect dominate in this momentum range.
- 20GeV-100GeV: The vertex with more layers has better d0 resolution, which is because vertex with more layers will have more measurement points for track reconstruction.

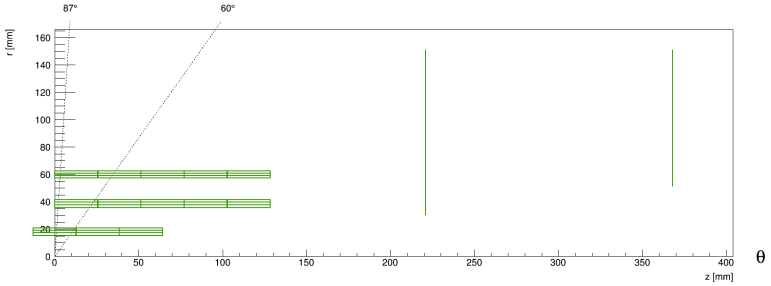

(a) RZ view of r=60mm

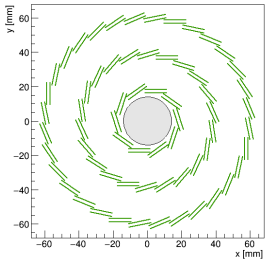

(b) XY view of r=60mm

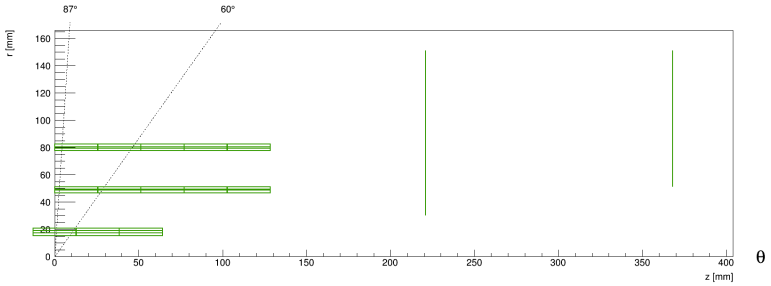

(c) RZ view of r=80mm

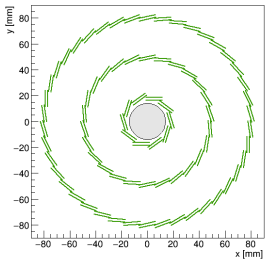

(d) XY view of r=80mm

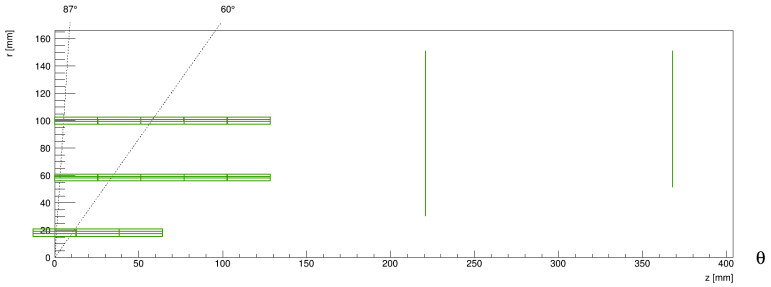

(e) RZ view of r=100mm

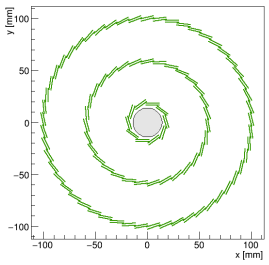

(f) XY view of r=100mm

Figure 6: RZ view and XY view for detector size of r=60mm ((a) and (b)), r=80mm ((c) and (d)) and r=80mm ((e) and (f).

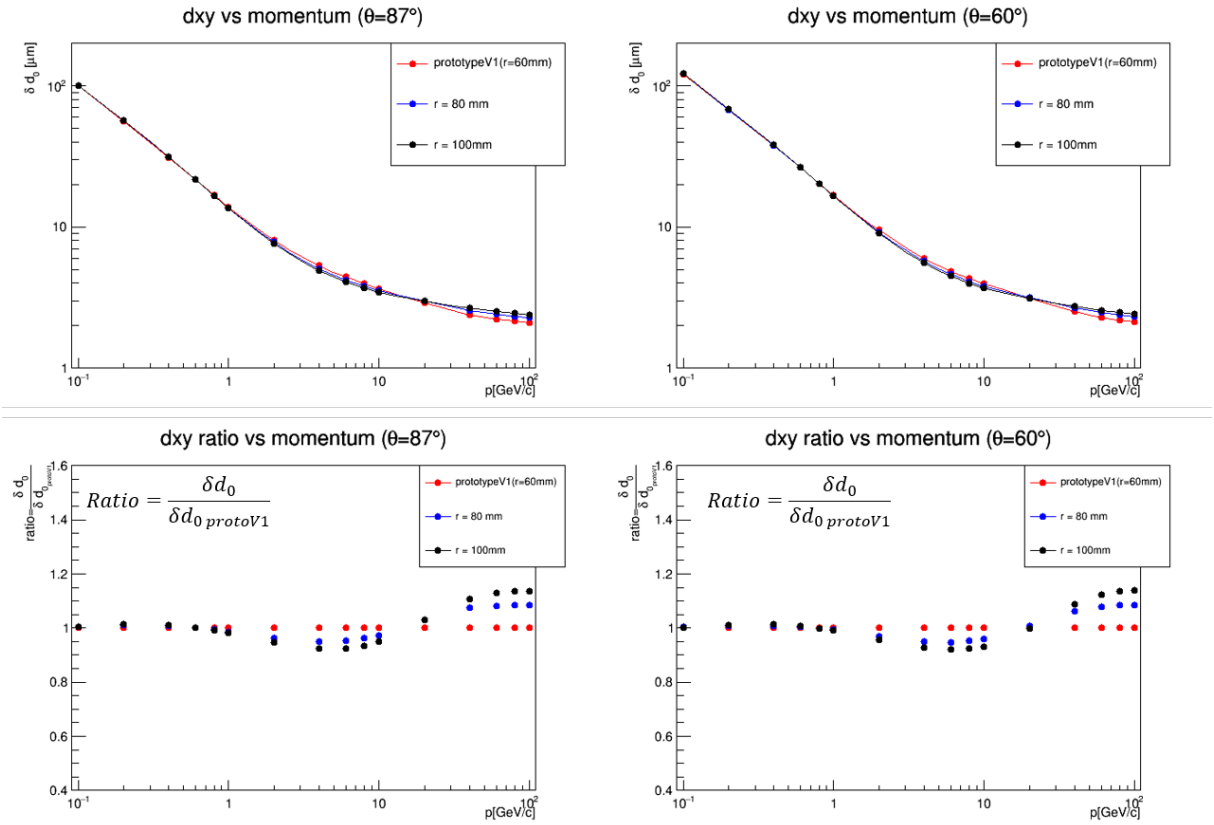

Figure 7: The d0 resolution, as a function of momentum, is compared for different detector size using single muon tracks with polar angle $\theta = 87°$ and 60°The d0 resolution, as a function of momentum, is compared for different detector size using single muon tracks with polar angle $\theta = 87°$ and 60°.

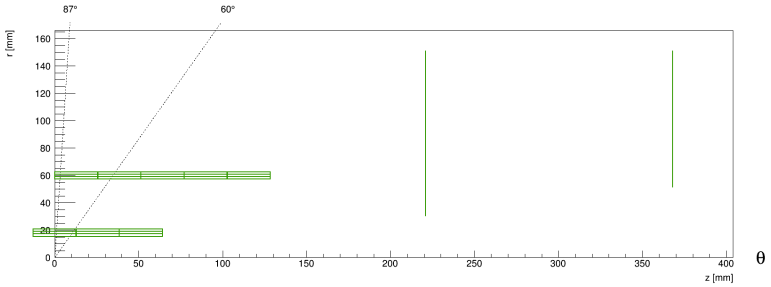

(a) RZ view of vertex with 2 layers

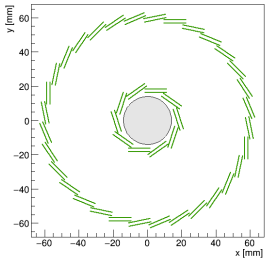

(b) XY view of vertex with 2 layers

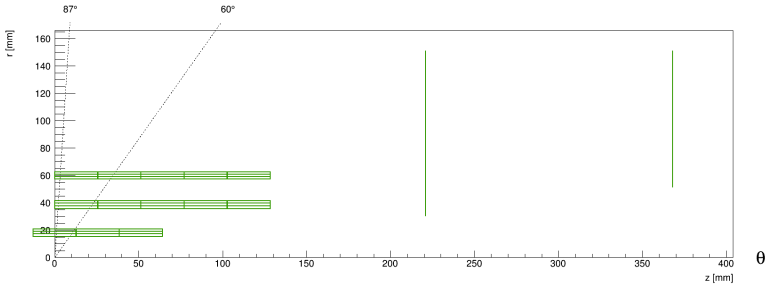

(c) RZ view of vertex with 3 layers

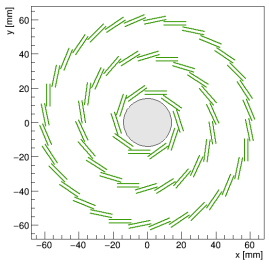

(d) XY view of vertex with 3 layers

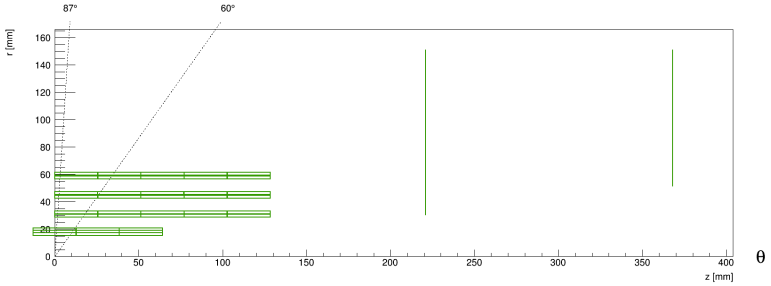

(e) RZ view of vertex with 4 layers

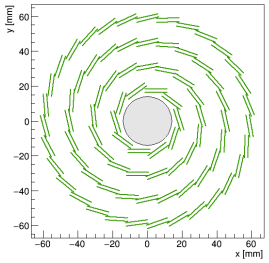

(f) XY view of vertex with 4 layers

Figure 8: RZ view and XY view of vertex layout with 2, 3 and 4 double-layers

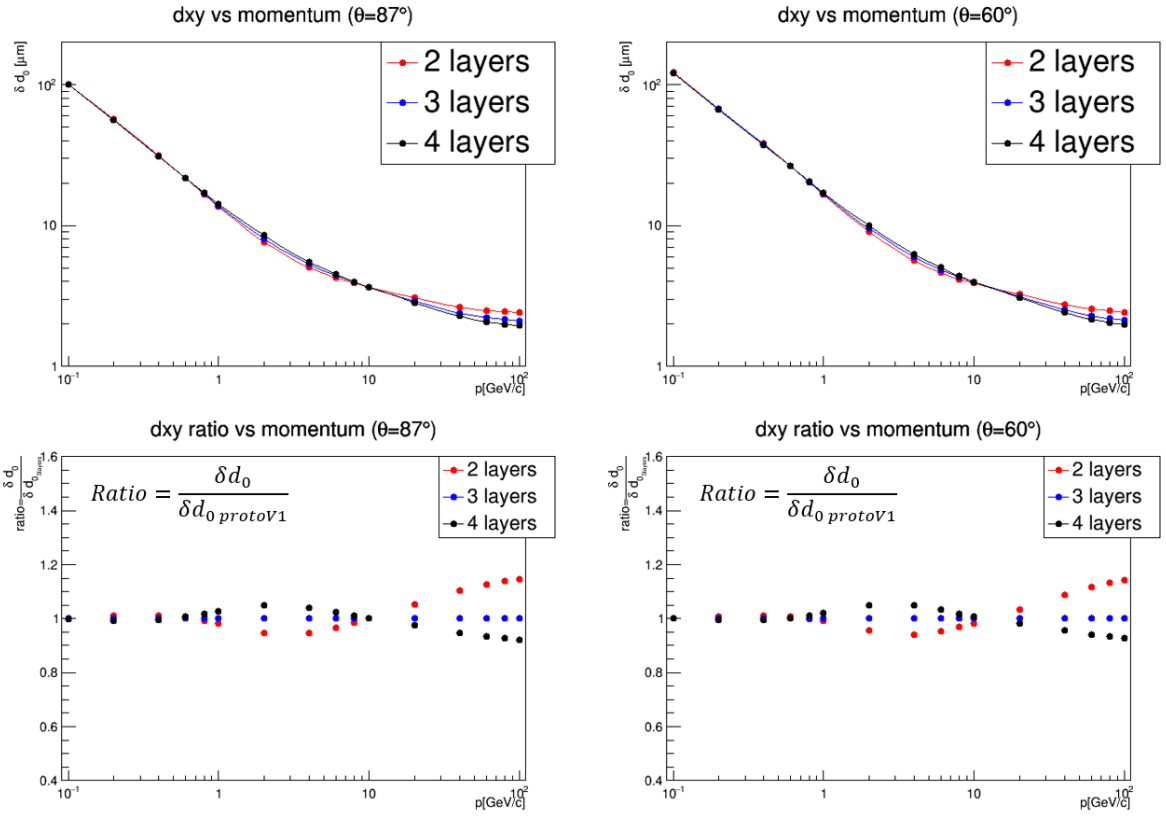

Figure 9: The d0 resolution, as a function of momentum, is compared for different detector size using single muon tracks with polar angle $\theta = 87°$ and 60°.

	2 layers	**3 layers**	**4 layers**
double-layer	R (mm)	R (mm)	R (mm)
Layer 1	18	18	18
Layer 2	60	38	31
Layer 3		60	45
Layer 4			60

Table 5: Double-layer radii for 2, 3 and 4 layers.

Finally, we study the effect of second layer radius on the transverse impact parameter resolution. We change the second layer radius by fixing the innermost layer and the outermost layer to study the variation of d0 resolution. The purpose of this study is to investigate how the d0 resolution varies when the vertex layers are not placed equidistantly. We study the d0 resolution for different second double layer radii every 7mm from 25mm to 53mm. The parameters of these layouts are given in Table 6and these layouts are shown in Figure 10.

	r_2**=25mm**	r_2**=32mm**	r_2**=39mm**	r_2**=46mm**	r_2**=53mm**
double-layer	R (mm)	R (mm)	R (mm)	R (mm)	R (mm)
Layer 1	18	18	18	18	18
Layer 2	25	32	39	46	53
Layer 3	60	60	60	60	60

Table 6: Double-layer radii for r_2=25, 32, 39, 46 and 53mm.

The d0 resolution, as a function of second layer radius is compared for momentum of 1GeV, 10GeV and 100GeV, using single muon tracks at polar angle $\theta = 87°$ and 60° in Figure 10. From the resolution plots we can conclude that second layer radius has very small effect on d0 resolution. In addition, second layer closer to first layer has better resolution for 10GeV and 100GeV tracks and second layer closer to first layer will get worse resolution for 1GeV tracks. However, second layer in middle is a better choice for mechanics design.

4.3 Long barrel vertex

In order to solve the air cooling issue, there is a proposal that we use a very long barrel without endcap. Without the endcap disk, the air can flow easily from one end of the detector to the other and take the heat away from the detector. Based on this new ideal, we make a long barrel vertex design whose layout is shown in Figure 12.

The long barrel vertex only contains three very long double pixel layer. The diameter of the first layer is 33*mm* and the length in +z direction is 130*mm*. The diameter of the second layer is 68*mm* and the length in +z direction is 255*mm*. The diameter of the third layer is 103*mm* and the length in +z direction is 380*mm*. The coverage of the long barrel vertex can reach polar angle $\theta = 8°$ and the radius of the whole detector is smaller than the prototype_v1. The detail parameters of the long barrel vertex are given in Table 7.

The d0 resolution, as a function of polar angle θ, is compared for different vertex layout (see Figure 13), using single muon tracks with momentum of 1GeV, 10GeV, 20GeV, 40GeV, 80GeV and 100GeV

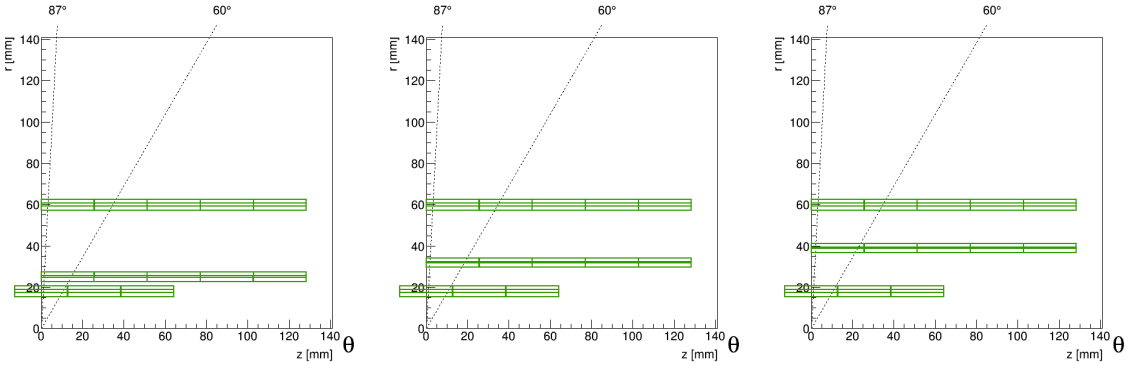

(a) RZ view of vertex barrel with r_2=25mm (b) RZ view of vertex barrel with r_2=32mm (c) RZ view of vertex barrel with r_2=39mm

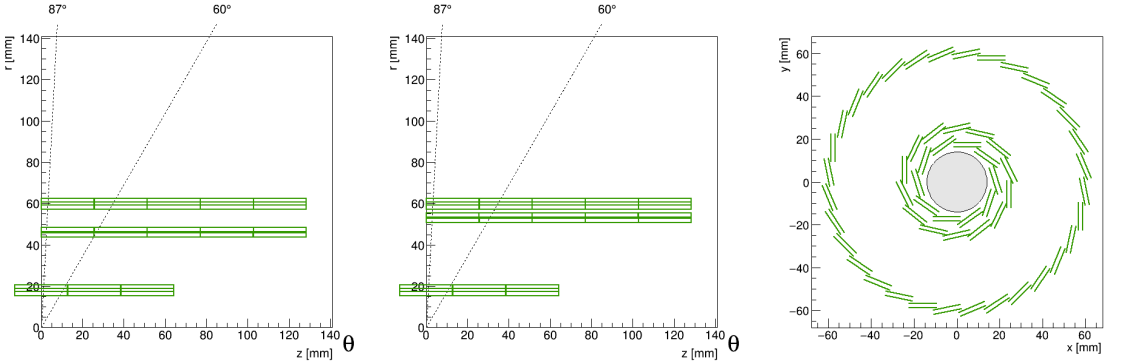

(d) RZ view of vertex barrel with r_2=46mm (e) RZ view of vertex barrel with r_2=53mm (f) XY view of vertex with r_2=25mm

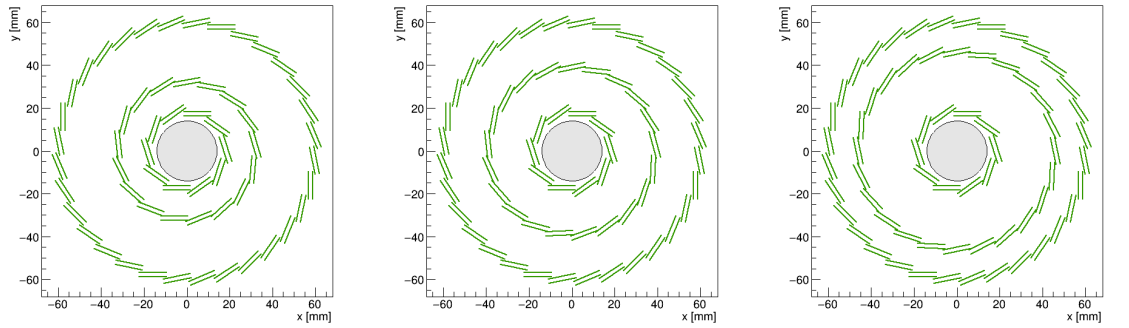

(g) XY view of vertex with r_2=32mm (h) XY view of vertex with r_2=39mm (i) XY view of vertex with r_2=46mm

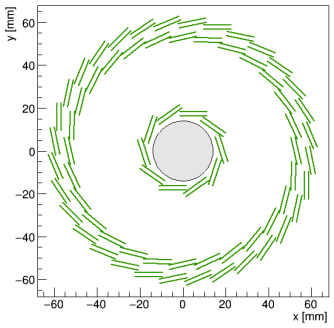

(j) XY view of vertex with r_2=53mm

Figure 10: RZ view and XY view of vertex layout with r_2=25mm, 32mm, 39mm, 46mm and 53mm.

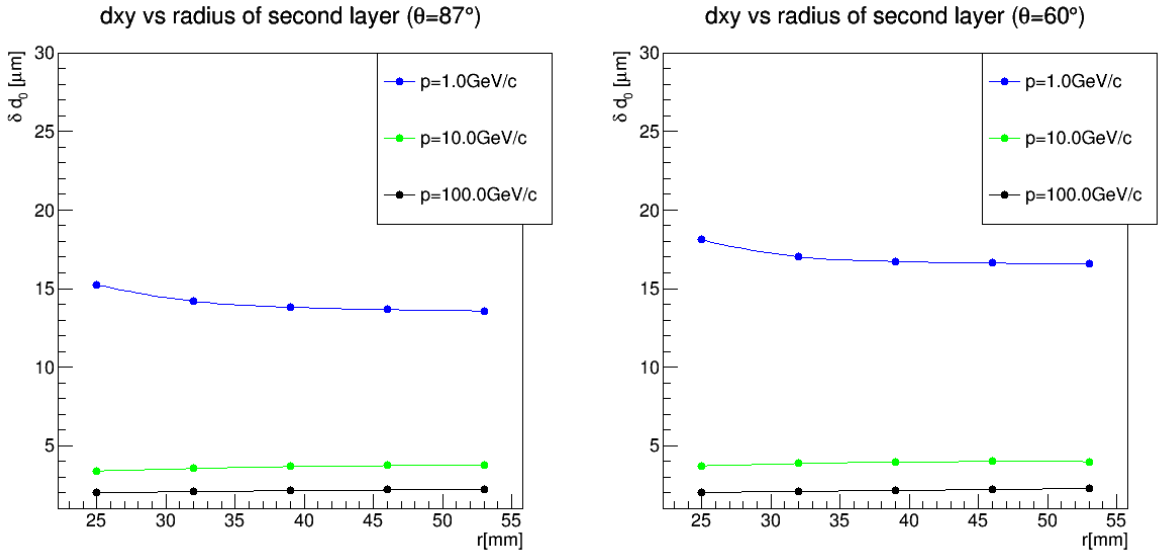

Figure 11: The d0 resolution, as a function of second layer radius is compared for momentum of 1GeV, 10GeV and 100GeV, using single muon tracks at polar angle $\theta = 87°$ and 60°.

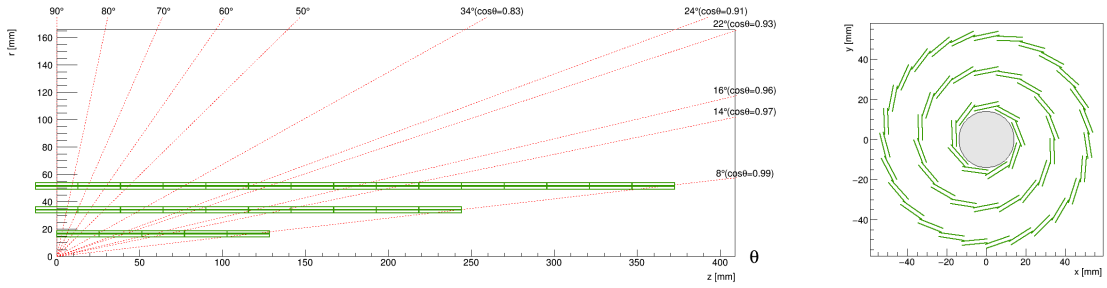

(a) RZ view of long barrel vertex

(b) XY view of long barrel vertex

Figure 12: Schematic layout of long barrel vertex in R-Z plane (a) and X-Y plane (b).

double layer	R (mm)	$\|z\|$ (mm)
Layer 1	16.50	128.45
Layer 2	34.00	244.10
Layer 3	51.50	372.40

Table 7: parameters for long barrel vertex. R represents the average radius of double layer, z the half length of the ladder in the layer.

in Figure 14. We can conclude that d0 resolution of long barrel vertex is always better than other two vertex designs which contain disk in low momentum region (p=1GeV, 10GeV and 20GeV), and in high momentum region (p=40GeV, 80GeV and 100GeV), d0 resolution of long barrel vertex is also better than other two vertex designs except θ from 16° to 34° due to number and position of measurement points. The material budget distribution by components of this ideal long barrel vertex is shown in Figure 15.

At first we use the same module as prototype_v1 for the long barrel vertex. However, due to this very long barrel, we must take into account the stiffness of the support in a real detector. Hence we redesign the ladder support by thickening the carbon fiber of the ladder support and increasing the height of the ladder support. In addition, with the length of the ladder increasing, the sensors in the ladder also increase, which means the requirements for the readout electronics become higher and more flex cable, whose material is also considered, is needed. This new long barrel vertex layout, called realistic long barrel vertex, is shown in Figure 16. The material budget of this realistic long barrel vertex is shown in Figure 17. We can see that the material of the realistic long barrel vertex increases about 100% comparing to ideal long barrel vertex.

4.4 Prototype_v1 layout optimization

Long barrel vertex has the advantage of simple structure and designing air cooling easily but the material budget increases sharply in the very front region (see Figure 12). That's why majority detector use the design with the endcaps instead of such a very simple long barrel design. With the development of CMOS technology, we are able to make sensors thin and read them efficiently, which makes the long barrel design possible. In order to improve the vertex performance as much as possible, we still want to optimize the prototype_v1 which contains endcap disk. The optimization can divide into two parts: barrel optimization and disk optimization.

4.4.1 barrel optimization

Firstly, we maintain the barrel design of the prototype_v1 and then consider different pixel disk design: 2 single disks, 2 double disks and 3 double disks. The layouts and parameters of these new vertex are given in Figure 18 and Table 8. In Figure 18, the black line inside the vertex barrel is the beam pipe and the blue line outside the vertex barrel is a carbon fiber tube to strengthen the support of the beam pipe.For 2 single disks, we directly use the CDR disk design. For 2 double disks, we just replace the single pixel module of single disk with double pixel module. The vertex with 3 double disks is the design that inserts a double disk in the middle of the 2 double disks.

The d0 resolution, as a function of $cos\theta$, is compared for different layouts using single muon tracks with p=50GeV in Figure 18. From the simulation result we can see:

- $cos\theta$ from 0.82 to 0.96, the vertex with disk has better d0 resolution than long barrel design.

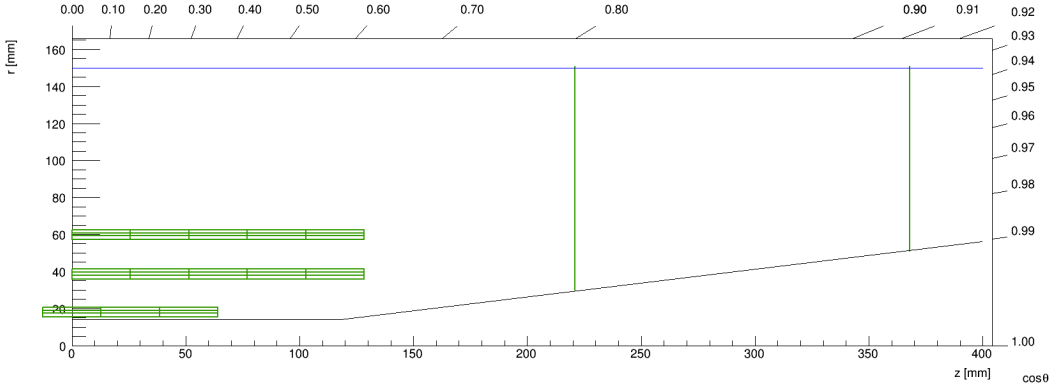

(a) RZ view of vertex layout containing prototype_v1 barrel and 2 single disks

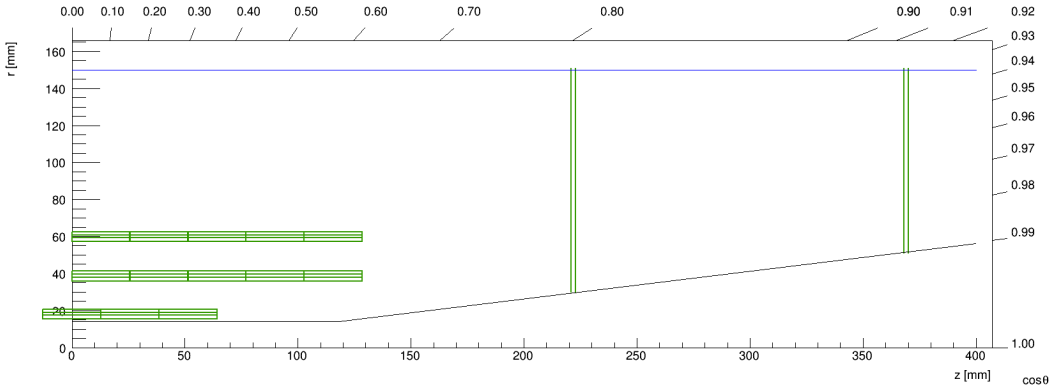

(b) RZ view of vertex layout containing prototype_v1 barrel and 2 double disks

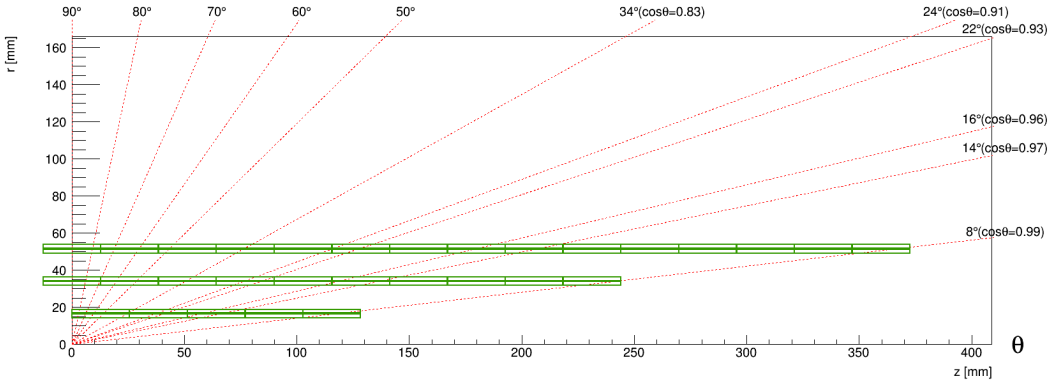

(c) RZ view of ideal long barrel vertex

Figure 13: RZ view of long barrel vertex (c) and vertex layout containing prototype_v1 barrel and 2 single disks (a) and 2 double disks (b).

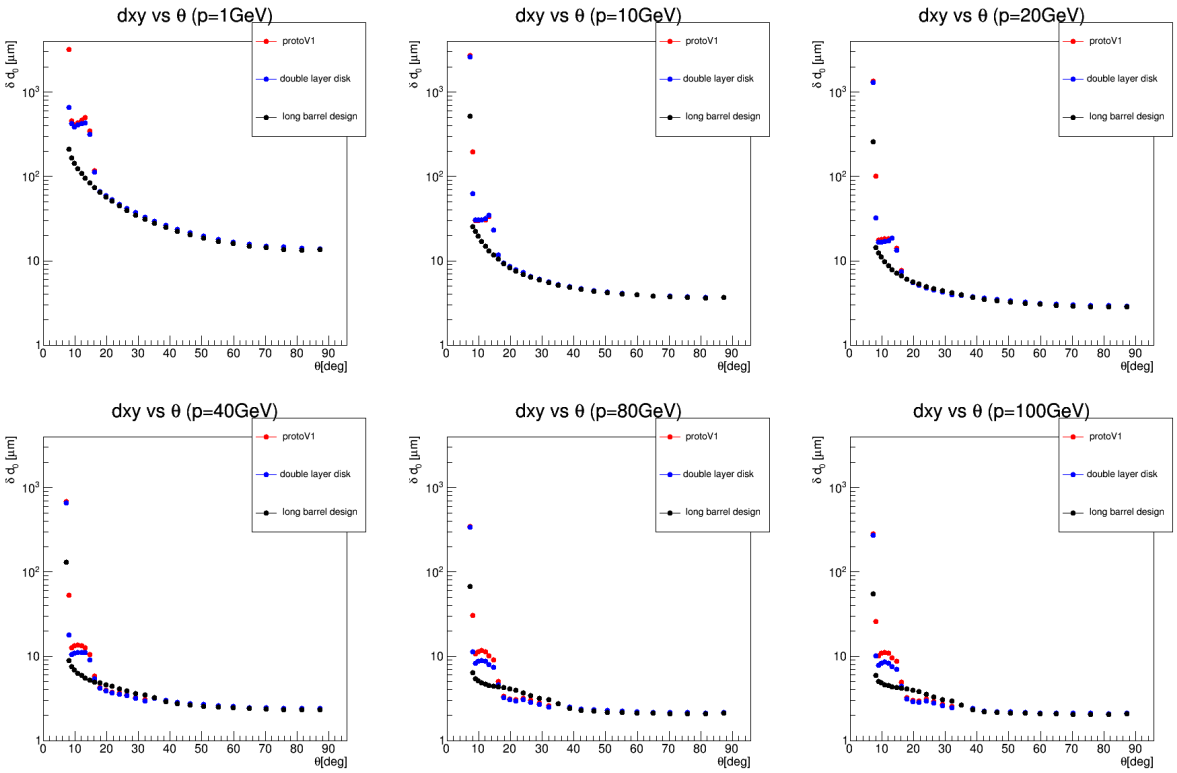

Figure 14: The d0 resolution, as a function of polar angle θ, is compared for different vertex layout (see Figure 13), using single muon tracks with momentum of 1GeV, 10GeV, 20GeV, 40GeV, 80GeV and 100GeV.

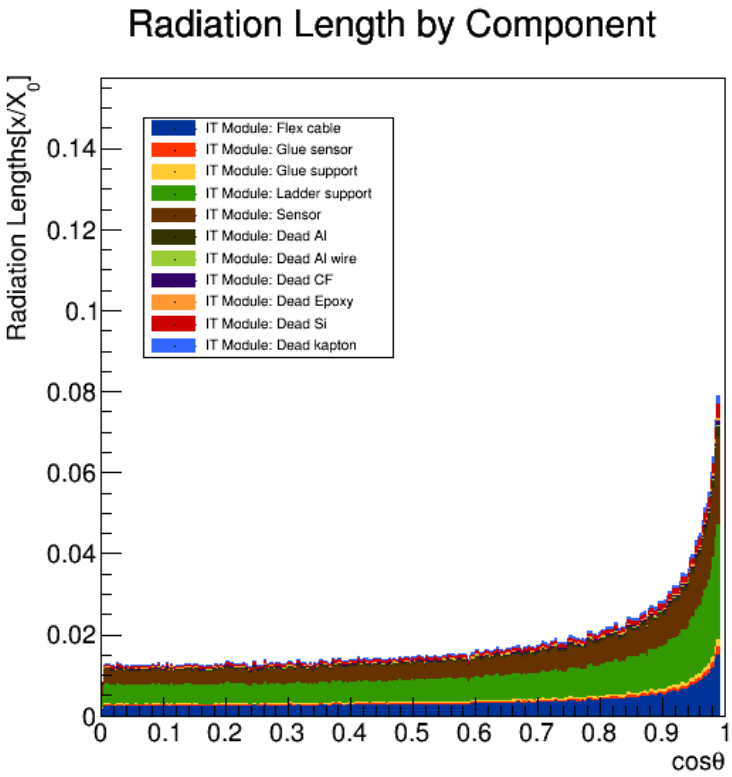

Figure 15: Material budget distribution of long barrel vertex by components.

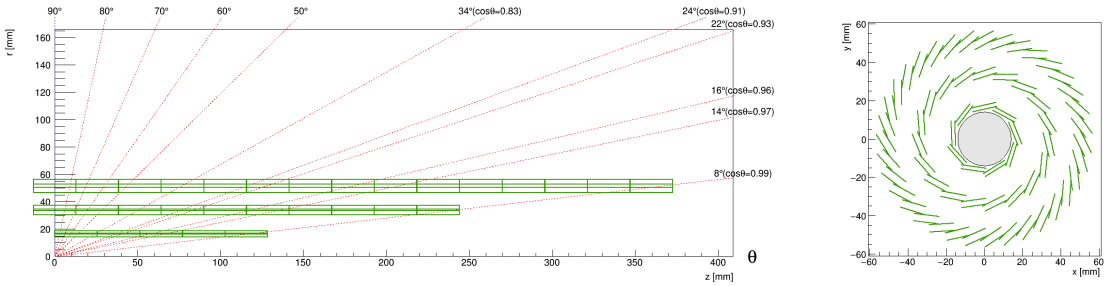

(a) RZ view of realistic long barrel vertex

(b) XY view of realistic long barrel vertex

Figure 16: Schematic layout of realistic long barrel vertex in R-Z plane (a) and X-Y plane (b).

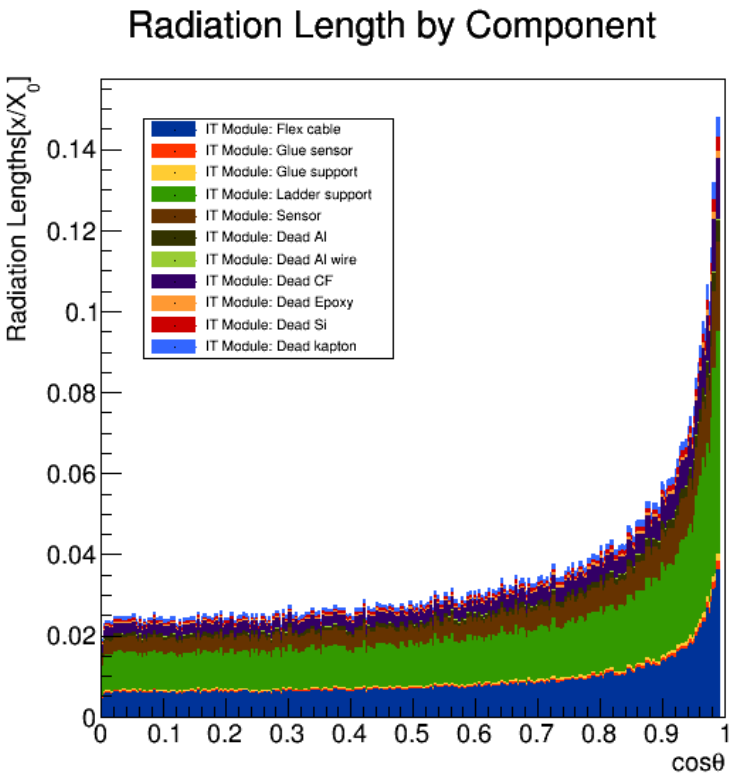

Figure 17: Material budget distribution of realistic long barrel vertex by components.

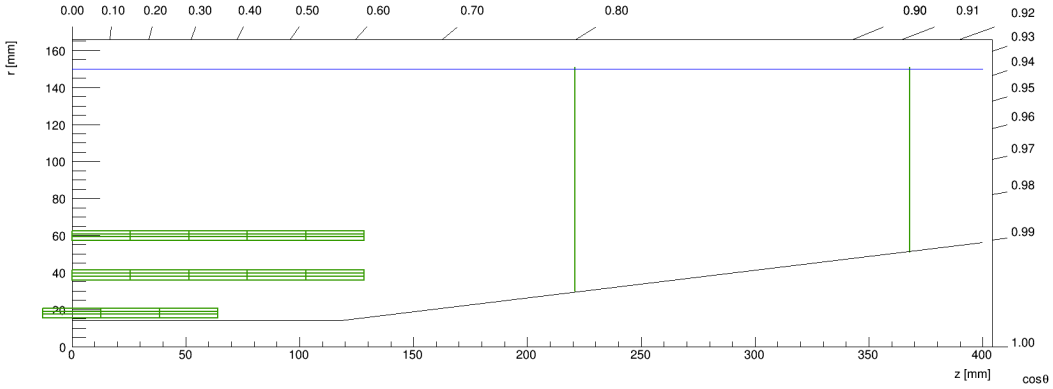

(a) RZ view of layout containing CDR barrel with 2 single disks

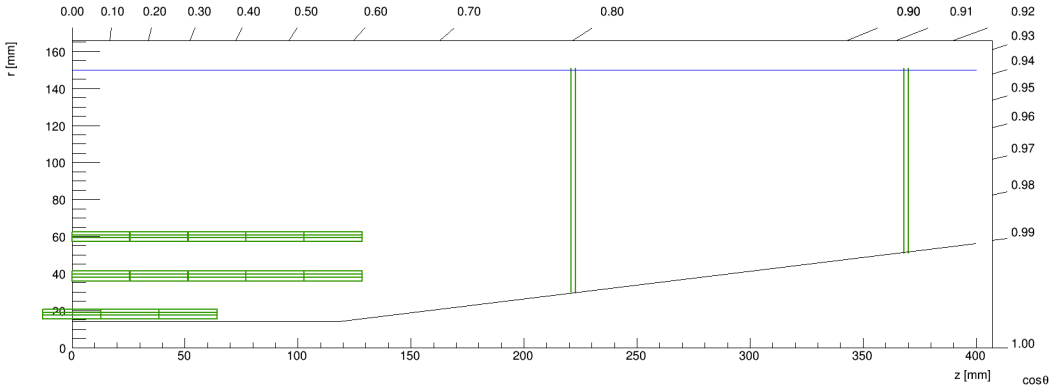

(b) RZ view of layout containing CDR barrel with 2 double disks

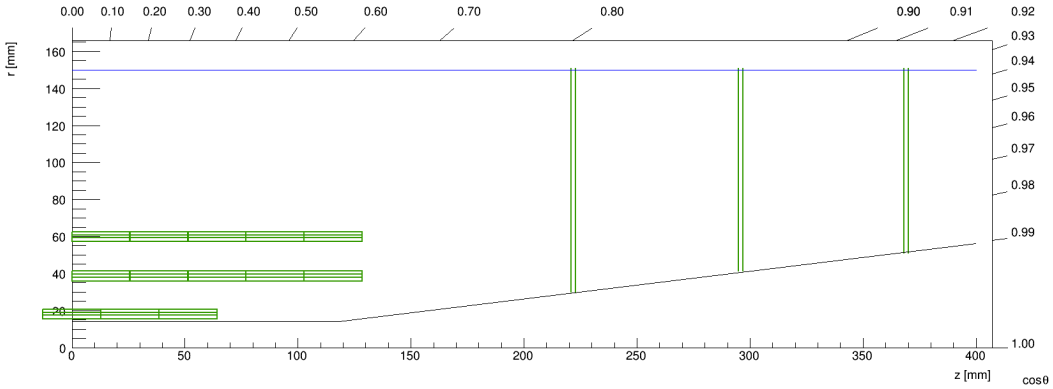

(c) RZ view of layout containing CDR barrel with 3 double disks

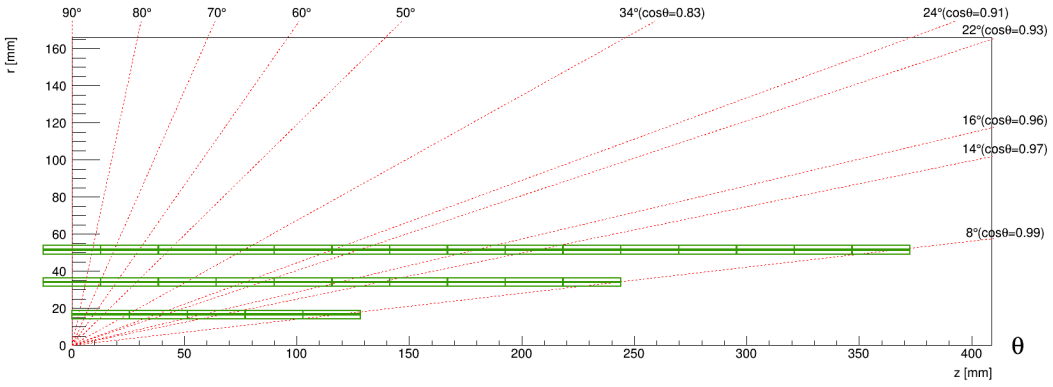

(d) RZ view of long barrel vertex layout

Figure 18: RZ view of different vertex layout which containing the CDR barrel but with different disk in endcap: 2 single disks (a), 2 double disks (b) and 3 double disks (c). RZ view of long barrel vertex layout is also shown in (d) as reference.

	2 single disks			2 double disks		
Barrel	R (mm)		$\pm z$ (mm)	R (mm)		$\pm z$ (mm)
Layer 1	18.00		64.20	18.00		64.20
Layer 2	38.00		128.45	38.00		128.45
Layer 3	60.00		128.45	60.00		128.45
Endcap	R_{in} (m)	R_{out} (m)	$\pm z$ (m)	R_{in} (m)	R_{out} (m)	$\pm z$ (m)
Disk 1	30.00	151.00	221.00	30.00	151.00	221.00
Disk 2	51.00	151.00	368.00	30.00	151.00	223.00
Disk 3				51.00	151.00	368.00
Disk 4				51.00	151.00	370.00

	3 double disks			long barrel vertex		
Barrel	R (mm)		$\pm z$ (mm)	R (mm)		$\pm z$ (mm)
Layer 1	18.00		64.20	16.50		128.45
Layer 2	38.00		128.45	34.00		244.10
Layer 3	60.00		128.45	51.50		372.60
Endcap	R_{in} (m)	R_{out} (m)	$\pm z$ (m)	R_{in} (m)	R_{out} (m)	$\pm z$ (m)
Disk 1	30.00	151.00	221.00			
Disk 2	30.00	151.00	223.00			
Disk 3	41.50	151.00	295.00			
Disk 4	41.50	151.00	297.00			
Disk 5	51.00	151.00	368.00			
Disk 6	51.00	151.00	370.00			

Table 8: Geometric parameters of vertex layouts containing CDR barrel and different disk in endcap: 2 single disks, 2 double disks and 3 double disks. The geometric parameters of long barre vertex is also given in this table. The barrel layers in this table are all double-layers.

- $cos\theta > 0.96$, the long barrel vertex has better resolution than the vertex containing CDR barrel and disk, which is because innermost layer of the long barrel vertex provides closer first hit to IP.

We find that the performance of the layout, only whose disk is optimized, is not better than the long barrel vertex, which makes us to optimize the barrel of prototype_v1 at the same time. From the study of long barrel vertex, we find the d0 resolution of long barrel vertex is always better than other vertex layouts with disk when $cos\theta$ is very small. The innermost layer of the long barrel vertex (128.45mm), covering the range of polar angle θ down to 8°, is longer than the innermost layer of prototype_v1 (64.20mm), which makes the first measurement point very close to the IP and hence makes the d0 resolution much better. Hence we maintain the second and third double layer of the prototype_v1 and then lengthen the first double layer to the same length of second and third layer, which is the same length as the first layer of long barrel vertex. The new vertex layout with longer first layer is shown in Figure 20 (b). It's endcap is the same as CDR with 2 single disks. The geometric parameters of this new layout and other 2 layouts are shown in Table 9.

From Figure 14 we can learn that the longer first layer of long barrel vertex improve the vertex d0 resolution a lot. Hence we optimize the barrel of the prototype_v1 by lengthening the first layer to the

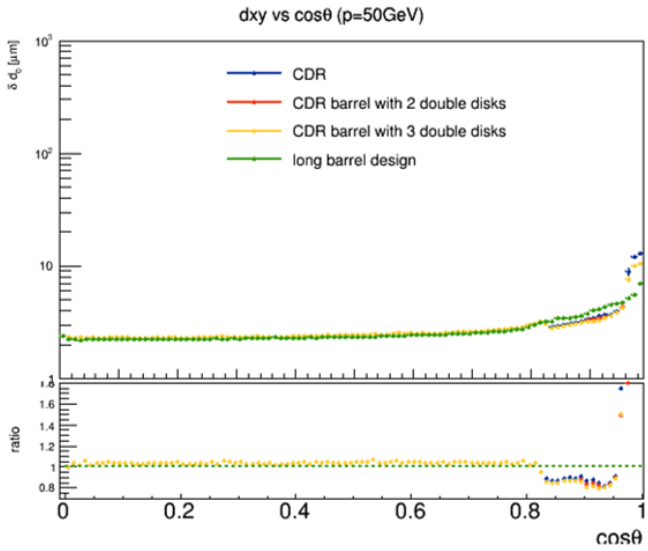

Figure 19: The d0 resolution, as a function of $cos\theta$, is compared for different layouts using single muon tracks with p=50GeV.

	CDR			**longer first layer**			**long barrel vertex**		
Barrel	R (mm)		$\pm z$ (mm)	R (mm)		$\pm z$ (mm)	R (mm)		$\pm z$ (mm)
Layer 1	18.00		64.20	18.00		128.45	16.50		128.45
Layer 2	38.00		128.45	38.00		128.45	34.00		244.10
Layer 3	60.00		128.45	60.00		128.45	51.50		372.60
Endcap	R_{in} (m)	R_{out} (m)	$\pm z$ (m)	R_{in} (m)	R_{out} (m)	$\pm z$ (m)	R_{in} (m)	R_{out} (m)	$\pm z$ (m)
Disk 1	30.00	151.00	221.00	30.00	151.00	221.00			
Disk 2	51.00	151.00	368.00	30.00	151.00	368.00			

Table 9: Geometric parameters of vertex layout with CDR barrel and 2 single disks, longer first layer with 2 single disks and long barrel vertex. The barrel layers in this table are all double-layers.

same as outer two layers. The d0 resolution, as a function of $cos\theta$, is compared for the new barrel with CDR endcap layout, CDR layout and long barrel vertex layout, using single muon tracks with momentum of 50GeV in Figure 21. All layouts are shown in Figure 20. From the simulation result we can conclude that longer first layer layout has the advantages of long barrel design and disk design because the d0 resolution of longer first layer is better than long barrel vertex and CDR at $cos\theta > 0.96$. Hence we choose this barrel with longer first layer as optimal vertex barrel.

4.4.2 disk optimization

After optimizing the vertex barrel, we want to optimize the disk in the endcap. Based on the optimized barrel, we investigate the effect of the putting place of the disk on the vertex transverse impact parameter. Here we consider four different layouts (see in Figure 22):

- CDR disk, as a reference.

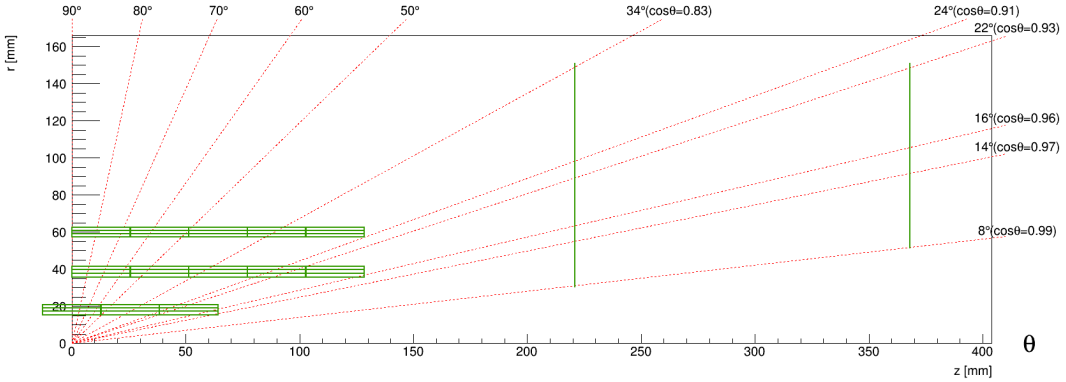

(a) RZ view of layout containing prototype_v1 barrel with CDR disk

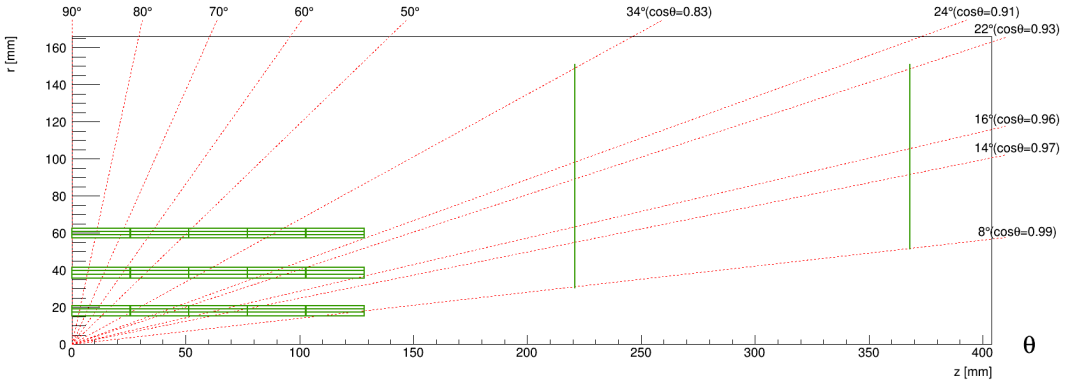

(b) RZ view of layout containing a longer first layer and 2 single disks

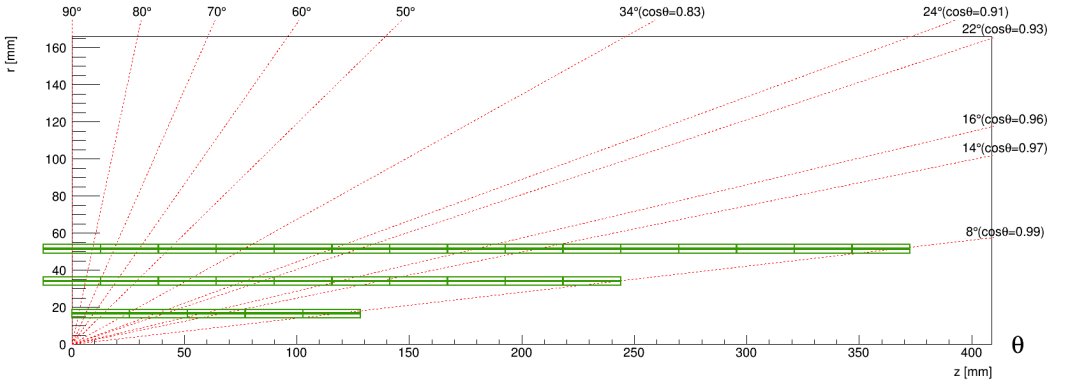

(c) RZ view of long barrel vertex layout

Figure 20: RZ view of 3 different layouts: prototype_v1 barrel with 2 single disks (a), longer first layer with 2 single disks (b) and long barrel vertex (c). The red dashed lines show the projection of μ track in $r-z$ plane, so you can count the number of hits the vertex detector will get when the μ shoot in this direction (for instance, there will be 6 hits information at polar angle θ=50°) in (b).

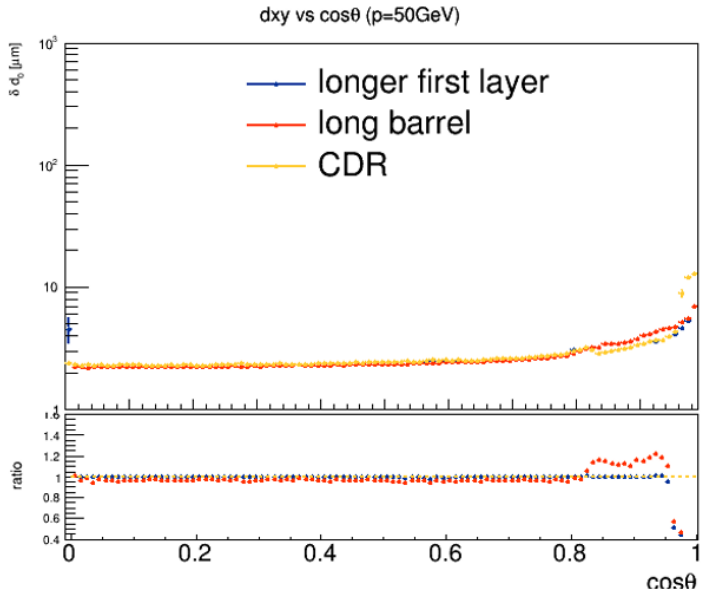

Figure 21: The d0 resolution, as a function of $cos\theta$, is compared for the new barrel with CDR endcap layout, CDR layout and long barrel vertex layout, using single muon tracks with momentum of 50GeV.

- Moving the first disk of the CDR disk toward the end of the barrel to a distance of 50mm, which is feasible for cable going out.
- Moving the two CDR disks toward the end of the barrel to a distance of 50mm.
- Moving the disk which is near the end of the barrel 50mm away from the barrel while fixing the outermost disk.

All the disk adjustment mentioned above should keep the inner ring of the disk not touching the line of polar angle $\theta = 8°$.

The geometric parameters of these 4 layouts are shown in Table 10. The d0 resolution, as a function of $cos\theta$, is compared for different layouts using single muon tracks with momentum of 50GeV in Figure 23. From the simulation result, we can conclude that no vertex layout which adjusts the disk putting place can improve the d0 resolution across all $cos\theta$, and the effect of the disk putting place on d0 resolution is very small.

Then we revisit the issue of the number of disk and choosing single or double disk. We take the new barrel to optimize the disk and then investigate three layouts:

- Vertex with 2 single disks in endcap and 3 same length double layer in barrel.
- Vertex with 2 double disks in endcap and 3 same length double layer in barrel.
- Vertex with 3 double disks in endcap and 3 same length double layer in barrel.

Figure 24 shows the layouts we investigate. Geometric parameters of these layouts are shown in Table 11. The d0 resolution, as a function of $cos\theta$, is compared for different layouts using single muon tracks with momentum of 50GeV in Figure 25. We can conclude that there are two ways to improve resolution: increasing the number of disk and replacing single disk with double disk. The vertex with 3 double disks has better d0 resolution in forward region, so we choose 3 double disks as the optimal endcap design.

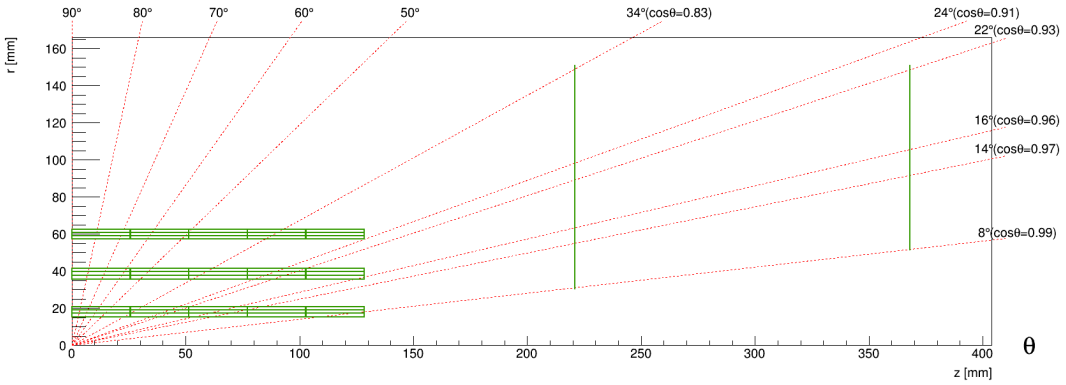

(a) RZ view of vertex layout containing longer first layer and CDR disk

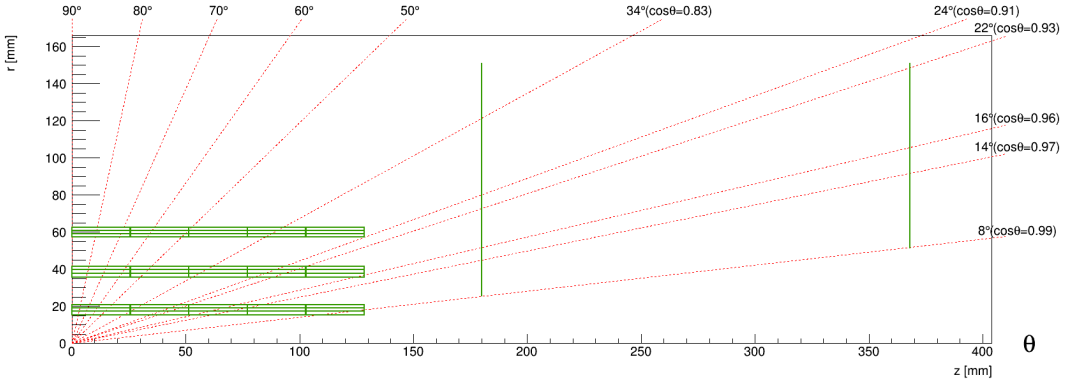

(b) RZ view of vertex layout containing longer first layer and closer first disk

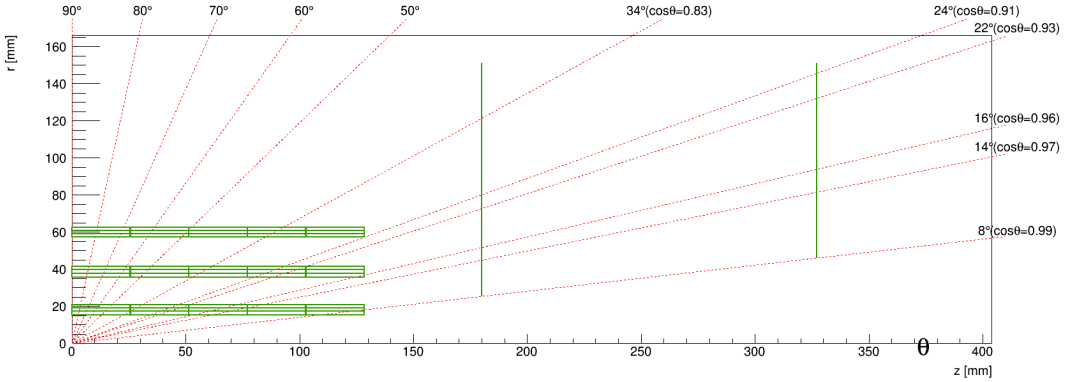

(c) RZ view of vertex layout containing longer first layer and 2 single disks closer to barrel

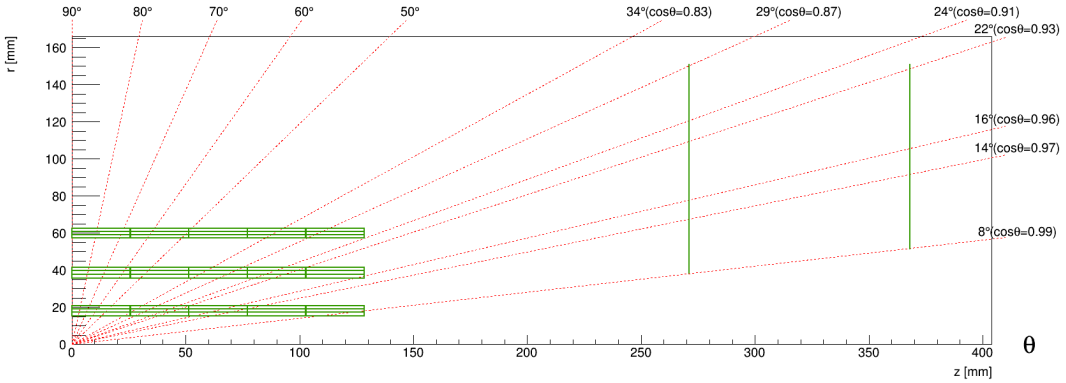

(d) RZ view of vertex layout containing longer first layer and first disk furth away barrel

Figure 22: RZ view of 4 vertex layouts we used to study the effect of disk putting place on the d0 resolution.

	CDR disk			closer first disk		
Barrel	R (mm)		$\pm z$ (mm)	R (mm)		$\pm z$ (mm)
Layer 1	18.00		128.45	18.00		128.45
Layer 2	38.00		128.45	38.00		128.45
Layer 3	60.00		128.45	60.00		128.45
Endcap	R_{in} (m)	R_{out} (m)	$\pm z$ (m)	R_{in} (m)	R_{out} (m)	$\pm z$ (m)
Disk 1	30.00	151.00	221.00	25.30	151.00	180.00
Disk 2	51.00	151.00	368.00	51.00	151.00	368.00

	closer 2 disks			further first disk		
Barrel	R (mm)		$\pm z$ (mm)	R (mm)		$\pm z$ (mm)
Layer 1	18.00		128.45	18.00		128.45
Layer 2	38.00		128.45	38.00		128.45
Layer 3	60.00		128.45	60.00		128.45
Endcap	R_{in} (m)	R_{out} (m)	$\pm z$ (m)	R_{in} (m)	R_{out} (m)	$\pm z$ (m)
Disk 1	25.30	151.00	180.00	38.00	151.00	271.00
Disk 2	45.90	151.00	327.00	51.00	151.00	368.00

Table 10: Geometric parameters of vertex layouts containing longer first layer and 2 single disks putting in different place: CDR disk, closer first disk, closer 2 disks and further first disk. The barrel layers in this table are all double-layers.

	2 single disks			2 double disks			3 double disks		
Barrel	R (mm)		$\pm z$ (mm)	R (mm)		$\pm z$ (mm)	R (mm)		$\pm z$ (mm)
Layer 1	18.00		128.45	18.00		128.45	18.00		128.45
Layer 2	38.00		128.45	38.00		128.45	38.00		128.45
Layer 3	60.00		128.45	60.00		128.45	60.00		128.45
Endcap	R_{in} (m)	R_{out} (m)	$\pm z$ (m)	R_{in} (m)	R_{out} (m)	$\pm z$ (m)	R_{in} (m)	R_{out} (m)	$\pm z$ (m)
Disk 1	30.00	151.00	221.00	30.00	151.00	221.00	30.00	151.00	221.00
Disk 2	51.00	151.00	368.00	30.00	151.00	223.00	30.00	151.00	223.00
Disk 3				51.00	151.00	368.00	41.50	151.00	295.00
Disk 4				51.00	151.00	370.00	41.50	151.00	297.00
Disk 5							51.00	151.00	368.00
Disk 6							51.00	151.00	370.00

Table 11: Geometric parameters of vertex layout with longer first layer in barrel and different disk in endcap: 2 single disks, 2 double disks and 3 double disks. The barrel layers in this table are all double-layers.

The simulation result shows that the vertex layout which contains 3 double disk in endcap and 3 same length double layer in barrel has better d0 resolution than others. Then we move the 3 double disks

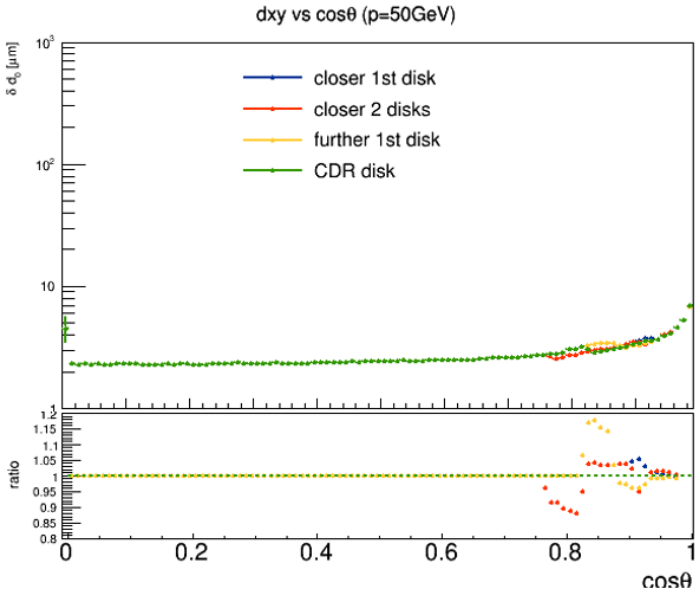

Figure 23: The d0 resolution, as a function of $cos\theta$, is compared for different layouts using single muon tracks with momentum of 50GeV.

toward the end of the barrel to the position where the distance between the innermost disk and barrel end is 50mm, to investigate the effect of the disk putting place on the the d0 resolution. Figure 26 shows the layouts. Geometric parameters of these studied layouts are shown in Table 12. The d0 resolution, as a function of $cos\theta$, is compared for different layouts using single muon tracks with momentum of 50GeV in Figure 27. The simulation results show that vertex which contains longer innermost layer and disk in endcap has better resolution than long barrel vertex in forward region. In addition, moving disk closer to barrel will enlarge the improved region. However, putting 3 double disk at CDR disk position is a better design considering the mechanics.

	long barrel vertex			**3 double disks**			**closer 3 double disks**		
Barrel	R (mm)		$\pm z$ (mm)	R (mm)		$\pm z$ (mm)	R (mm)		$\pm z$ (mm)
Layer 1	16.50		128.45	18.00		128.45	18.00		128.45
Layer 2	34.00		244.10	38.00		128.45	38.00		128.45
Layer 3	51.50		372.60	60.00		128.45	60.00		128.45
Endcap	R_{in} (m)	R_{out} (m)	$\pm z$ (m)	R_{in} (m)	R_{out} (m)	$\pm z$ (m)	R_{in} (m)	R_{out} (m)	$\pm z$ (m)
Disk 1				30.00	151.00	221.00	25.30	151.00	180.00
Disk 2				30.00	151.00	223.00	25.30	151.00	182.00
Disk 3				41.50	151.00	295.00	35.70	151.00	254.00
Disk 4				41.50	151.00	297.00	35.70	151.00	256.00
Disk 5				51.00	151.00	368.00	45.90	151.00	327.00
Disk 6				51.00	151.00	370.00	45.90	151.00	329.00

Table 12: Geometric parameters of long barrel vertex and vertex layout with longer first layer in barrel and different disk in endcap: 3 double disks and closer 3 double disks. The barrel layers in this table are all double-layers.

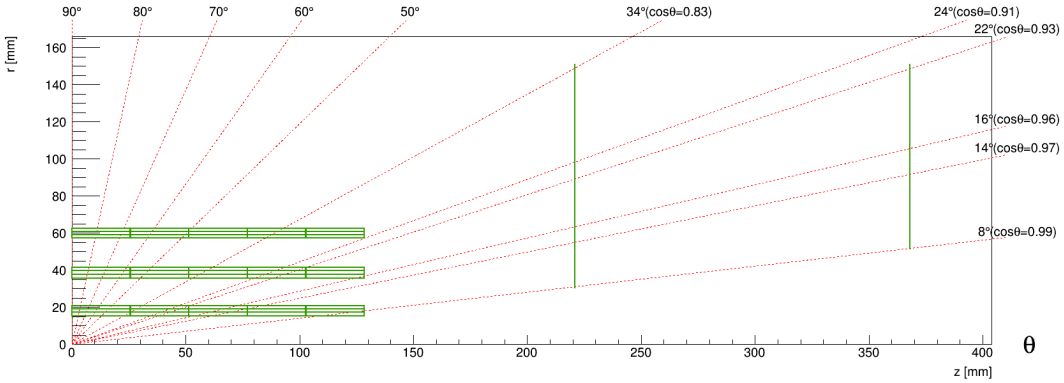

(a) RZ view of vertex layout containing longer first layer and 2 single disks

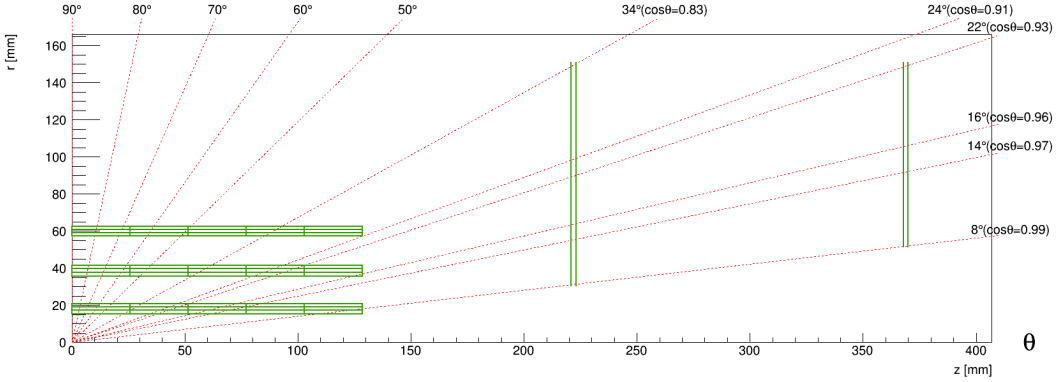

(b) RZ view of vertex layout containing longer first layer and 2 double disks

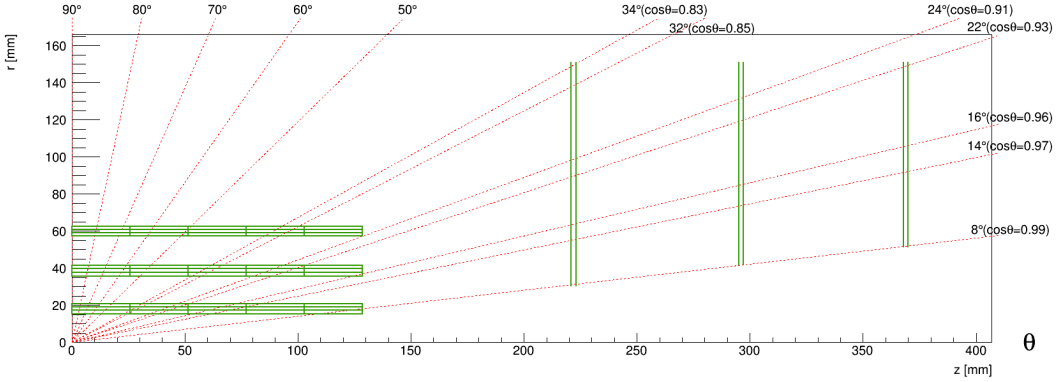

(c) RZ view of vertex layout containing longer first layer and 3 double disks

Figure 24: RZ view of vertex layout containing longer first layer and different disk in endcap: 2 single disks, 2 double disks and 3 double disks.

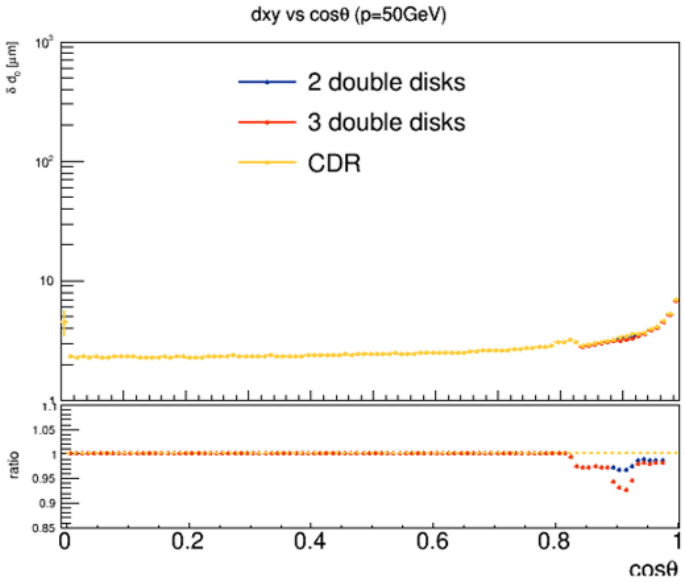

Figure 25: The d0 resolution, as a function of $cos\theta$, is compared for different layouts using single muon tracks with momentum of 50GeV.

In summary, we get an optimal vertex layout, three same length barrel layer with three double disks. The d0 resolution, as a function of $cos\theta$, is compared for three kinds of layouts, CDR, long barrel vertex and optimal layout, using single muon tracks with momentum of 50GeV in Figure 28. The results show that the performance of the optimal layout is better than long barrel vertex because of combination of longer first layer, having the advantage of long barrel vertex, and disk which has lower material budget and more measurement points in forward region.

4.5 New disk arrangements investigation

In section 4.4, considering d0 resolution as criteria, we get an ideal optimal layout which do not think about the mechanics and air cooling which is essentially important for reducing vertex material budget. Now there are already two choices for air cooling: one is the long barrel vertex without disk, the material budget of which will increase sharply in the forward region; another is the CLIC spiral disk concept [2] (see Figure 29), by rotating disk petals at fixed angle to create a spiral duct, which can also be applied to CEPC.

In this subsection, we want to make a new disk design satisfying all physics performance requirement and providing a path for air to flow through the detector. Here we cut all disks into two parts, then rearrange all disk parts to fulfill detector coverage and measurement points. Figure 30 shows all layouts we investigate. Geometric parameters of these new layouts are shown in Table13. The first layout is very similar to the second, in that a set of rings is moved as a whole so that the two parts of the disk are staggered to leave space for air flow. The first is to move the upper half of the rings closer to the barrel, and the second is to move the lower half of the rings closer to the barrel. The third option is to directly cut a ring of the same width in the middle of each disk, and then rearrange the remaining rings so that each particle emitted from IP can still pass through at least three disks in endcap region. The d0 resolution, as a function of $cos\theta$, is compared for different disk arrangements layout and vertex with 3 double disks, using single muon tracks with momentum of 50GeV in Figure 31.

The results show that the d0 resolution of these vertex layouts with new disk arrangements does not become much worse. For instance, the d0 resolution of the vertex which has hole in the middle

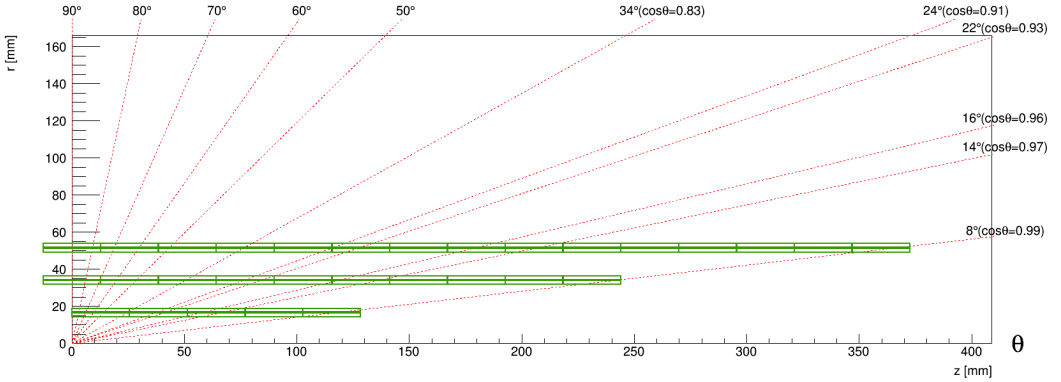

(a) RZ view of long barrel vertex layout

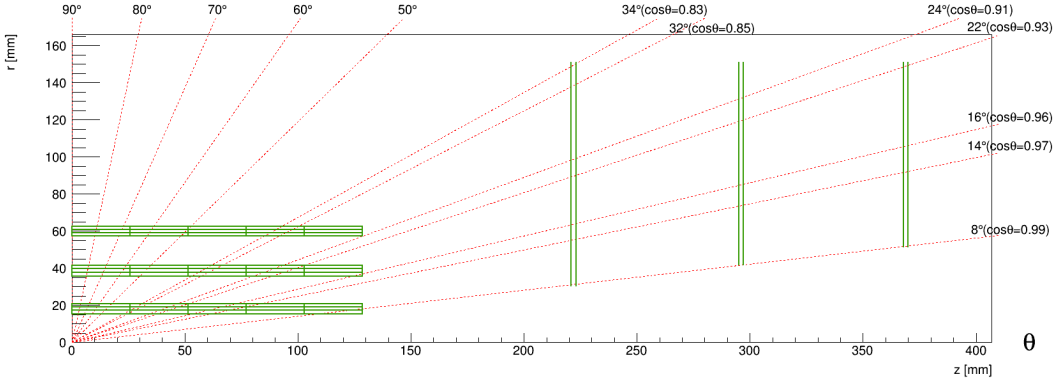

(b) RZ view of vertex layout containing longer first layer and 3 double disks

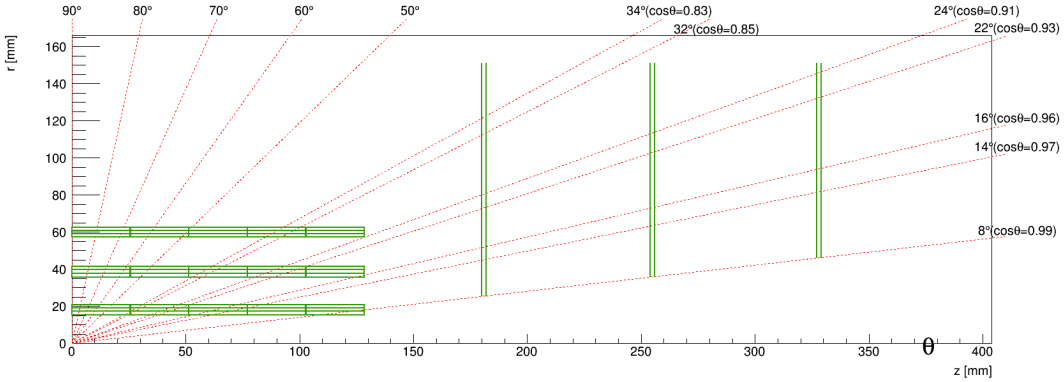

(c) RZ view of vertex layout containing longer first layer and closer 3 double disks

Figure 26: RZ view of different vertex layouts: long barrel vertex layout(a), vertex layout containing longer first layer and 3 double disks (b) and vertex layout containing longer first layer and closer 3 double disks (c).

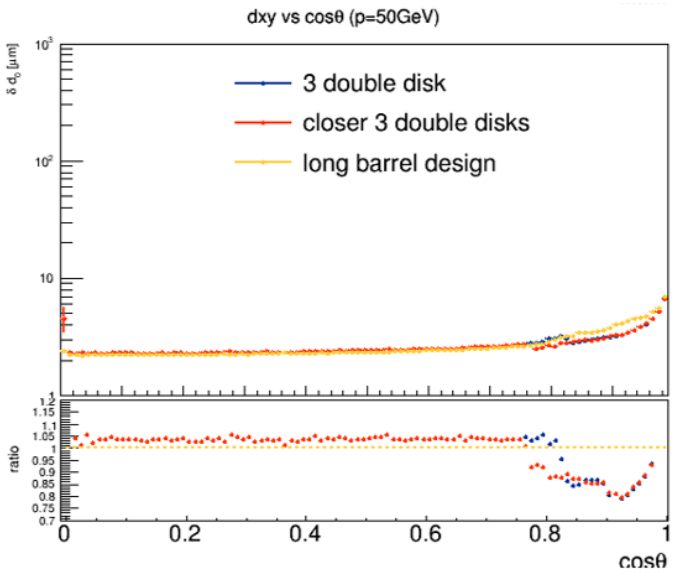

Figure 27: The d0 resolution, as a function of $cos\theta$, is compared for different layouts using single muon tracks with momentum of 50GeV.

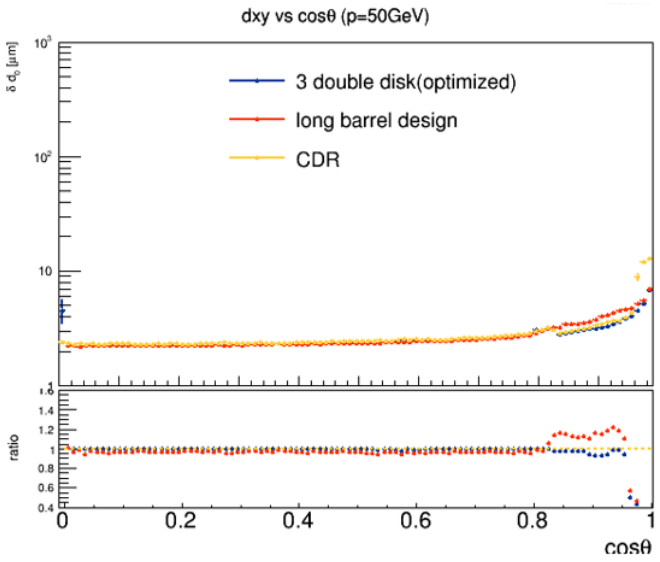

Figure 28: The d0 resolution, as a function of $cos\theta$, is compared for three kinds of layouts, CDR, long barrel vertex and optimal layout, using single muon tracks with momentum of 50GeV.

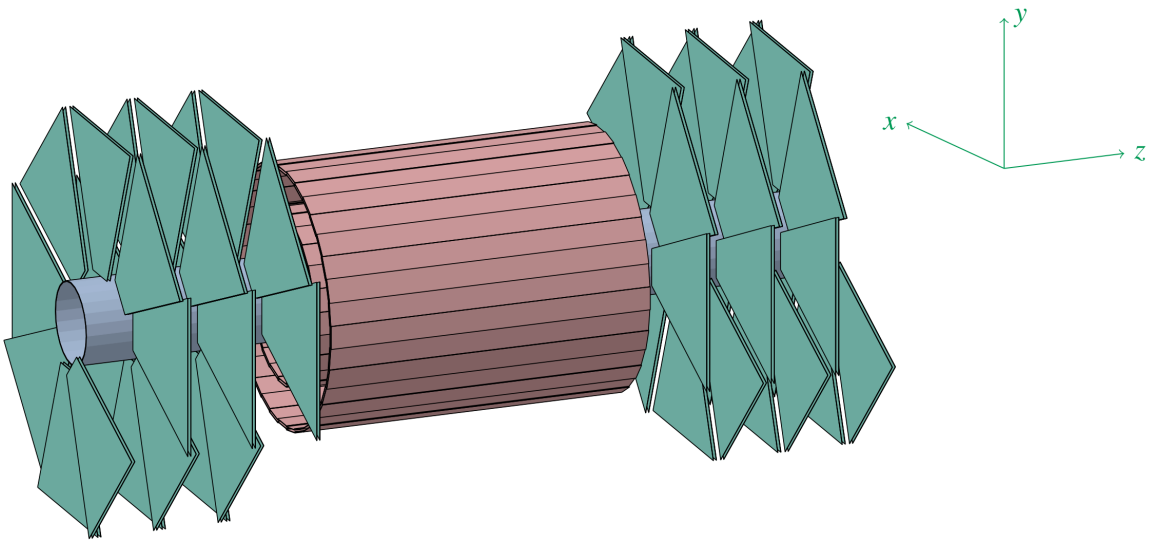

Figure 29: Schematic view of the CLIC spiral vertex concept geometry. The barrel region is shown in red and the vertex endcaps in green.

of disk, only decrease 15% at $cos\theta = 0.85$, due to measurement points farther away the IP. The d0 resolution decreases no more than 5% in other region even increases in some regions, which proves the new disk arrangements have very small effect on the vertex d0 resolution. But we still need to consider the mechanics for the new disk arrangements.

4.6 Beam pipe study

4.6.1 Beam pipe radius simulation

The first layer is directly mount on the beam pipe in current vertex mechanics design, hence smaller beam pipe radius leads to smaller radius of the vertex innermost layer, which will make the d0 resolution better because of first measurement point closer to IP. In this section, we study the d0 resolution of the vertex with the beam pipe radius of 10mm, 12mm, 14mm, 16mm. Figure 32 shows the layouts. The d0 resolution, as a function of momentum, is compared for different beam pipe radius using single muon tracks at polar angle $\theta = 85^\circ$ and 60° in Figure 33. We can conclude that:

- the effect of beam pipe radius on d0 resolution is very big for low momentum tracks.
- the beam pipe radius is smaller, the d0 resolution is better.
- the d0 resolution will improve 21% if the beam pipe radius reduce to 10mm.

4.6.2 Beam pipe material simulation

In order to cool down the beam pipe more efficient, we design a new beam pipe which contains two Beryllium layers and coolant is inside the gap of two layers (inner Beryllium thickness is 500um and outer Beryllium thickness is 350um). In order to reduce the beam γ backgroud, a 5um gold film is coated inside the beam pipe. This beam pipe is different from the CDR beam pipe design which only has one 500um Beryllium layer. So we compare the d0 resolution differences of the CDR beam pipe design to the new beam pipe design whose coolant includes paraffin and Helium gas which has the lowest material

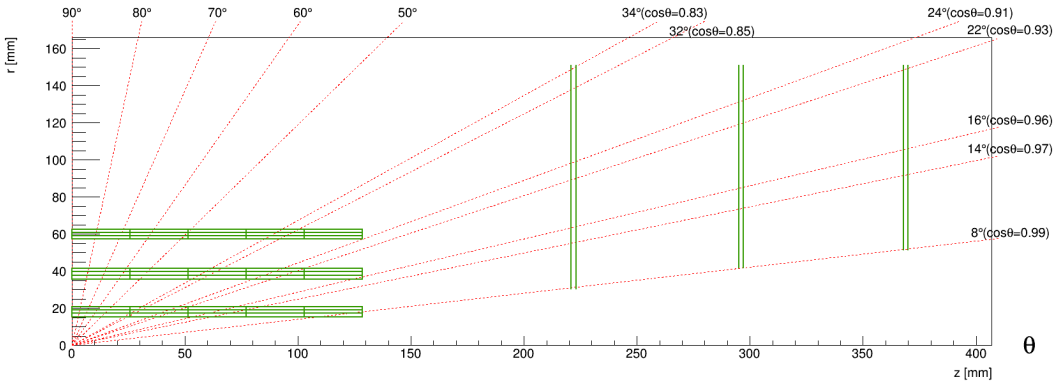

(a) RZ view of vertex layout containing longer first layer and 3 double disks

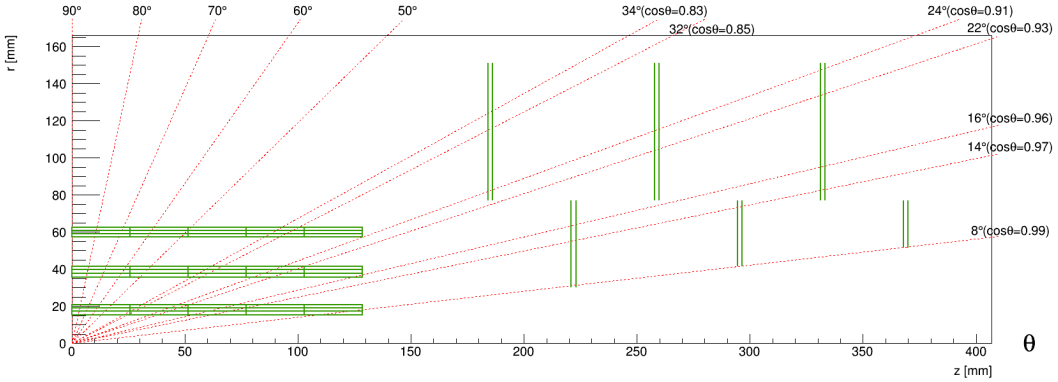

(b) RZ view of vertex layout containing longer first layer and upper ring set closer to barrel

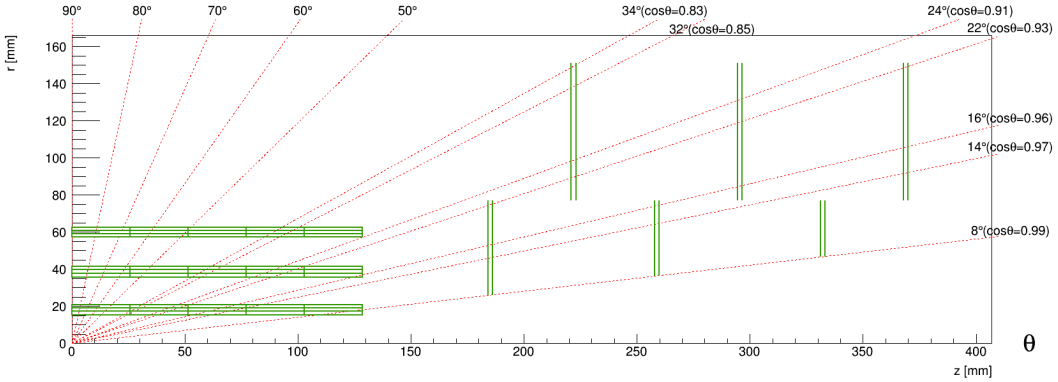

(c) RZ view of vertex layout containing longer first layer and lower ring set closer to barrel

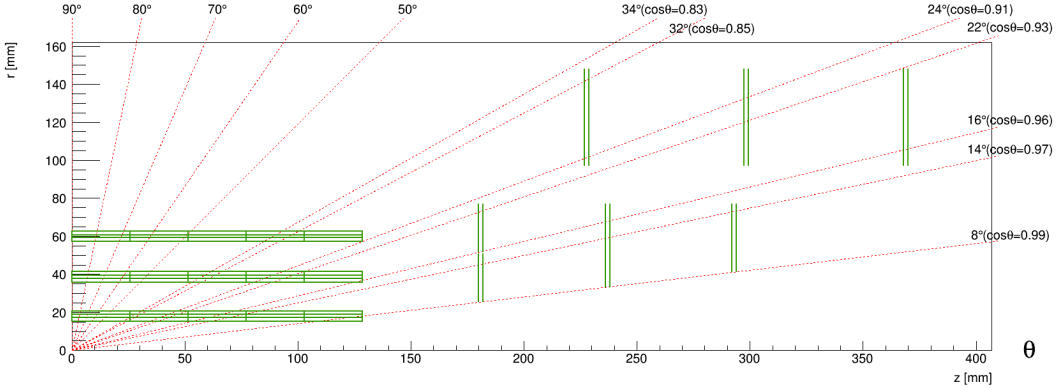

(d) RZ view of vertex layout containing longer first layer and a 20mm hole in endcap

Figure 30: RZ view of vertex layout containing longer first layer and endcap: 3 double layer disks (a), upper ring set closer to barrel (b), lower ring set closer to barrel (c) and 20mm ring hole (d).

	3 double disks			upper closer to barrel		
Barrel	R (mm)		±z (mm)	R (mm)		±z (mm)
Layer 1	18.00		128.45	18.00		128.45
Layer 2	38.00		128.45	38.00		128.45
Layer 3	60.00		128.45	60.00		128.45
Endcap	R_{in} (m)	R_{out} (m)	±z (m)	R_{in} (m)	R_{out} (m)	±z (m)
Disk 1	30.00	151.00	221.00	77.00	151.00	184.25
Disk 2	30.00	151.00	223.00	77.00	151.00	186.25
Disk 3	41.50	151.00	295.00	30.00	77.00	221.00
Disk 4	41.50	151.00	297.00	30.00	77.00	223.00
Disk 5	51.00	151.00	368.00	77.00	151.00	257.75
Disk 6	51.00	151.00	370.00	77.00	151.00	359.75
Disk 7				41.40	77.00	294.50
Disk 8				41.40	77.00	296.50
Disk 9				77.00	151.00	331.25
Disk 10				77.00	151.00	333.25
Disk 11				51.40	77.00	368.00
Disk 12				51.40	77.00	370.00

	lower closer to barrel			20mm ring hole		
Barrel	R (mm)		±z (mm)	R (mm)		±z (mm)
Layer 1	18.00		128.45	18.00		128.45
Layer 2	38.00		128.45	38.00		128.45
Layer 3	60.00		128.45	60.00		128.45
Endcap	R_{in} (m)	R_{out} (m)	±z (m)	R_{in} (m)	R_{out} (m)	±z (m)
Disk 1	25.90	77.00	184.25	25.30	77.00	180.00
Disk 2	25.90	77.00	186.25	25.30	77.00	182.00
Disk 3	77.00	151.00	221.00	97.00	148.20	226.80
Disk 4	77.00	151.00	223.00	97.00	148.20	228.80
Disk 5	36.20	77.00	257.75	33.20	77.00	236.05
Disk 6	36.20	77.00	359.75	33.20	77.00	238.05
Disk 7	77.00	151.00	294.50	41.00	77.00	292.10
Disk 8	77.00	151.00	296.50	41.00	77.00	294.10
Disk 9	46.60	77.00	331.25	97.00	148.20	297.40
Disk 10	46.60	77.00	333.25	97.00	148.20	299.40
Disk 11	77.00	151.00	368.00	97.00	148.20	368.00
Disk 12	77.00	151.00	370.00	97.00	148.20	370.00

Table 13: Geometric parameters of vertex layouts containing longer first layer and 2 single disks putting in different place: CDR disk, closer first disk, closer 2 disks and further first disk. The barrel layers in this table are all double-layers.

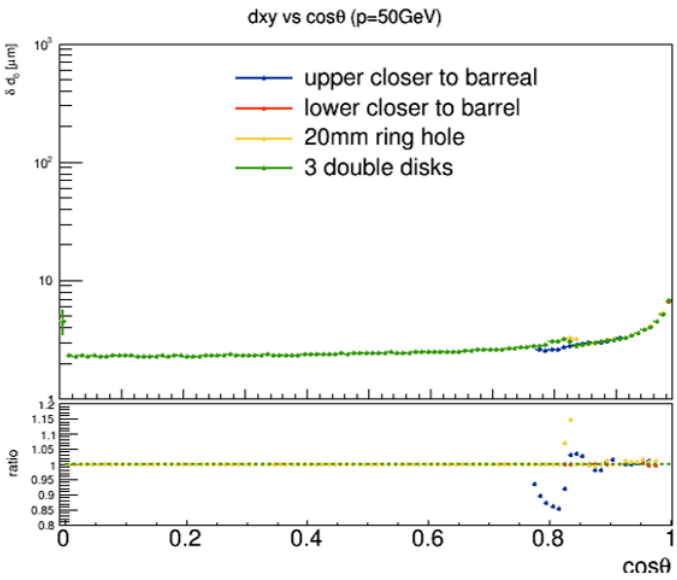

Figure 31: The d0 resolution, as a function of $cos\theta$, is compared for different disk arrangements layout and vertex with 3 double disks, using single muon tracks with momentum of 50GeV.

budget. The material budget of these three beam pipe design is directly calculated in Table 14. We only need to modify the x/X_0 value of beam pipe in the source code and then recompile to simply simulate the effect of beam pipe material on d0 resolution. Figure 34 shows the distribution of radiation length for different beam pipe design. The average value of radiation length for each components is given in Table 15. The d0 resolution, as a function of momentum, is compared for optimal layout with different beam pipe design, using single muon tracks at polar angle $\theta = 85°$ and $60°$ in Figure 35. We can conclude that the d0 resolution will be worse about 24% for 1GeV track if we use paraffin coolant.

	CDR	Helium gas coolant	Paraffin coolant
Au	0	0.001495	0.001495
Beryllium	0.001417	0.002409	0.002409
coolant	0	0	0.001037
total	0.001417	0.003905	0.004941

Table 14: Beam pipe material of each component for different design: CDR, Helium gas coolant design and paraffin coolant design.

5 Demonstration of performance

...

6 Summary and discussion

A customized silicon tracker fast simulation tool developed for CMS silicon tracker optimization can be used for CEPC vertex layout optimization and future full silicon tracker optimization. This tool can

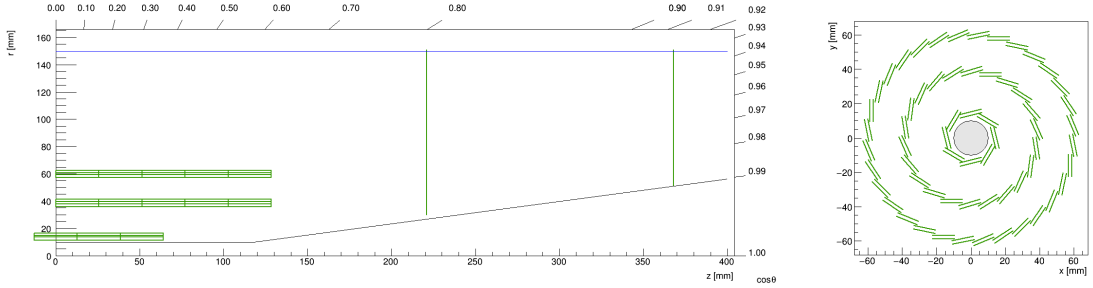

(a) RZ (left) and XY (right) view of vertex layout with beam pipe radius=10mm

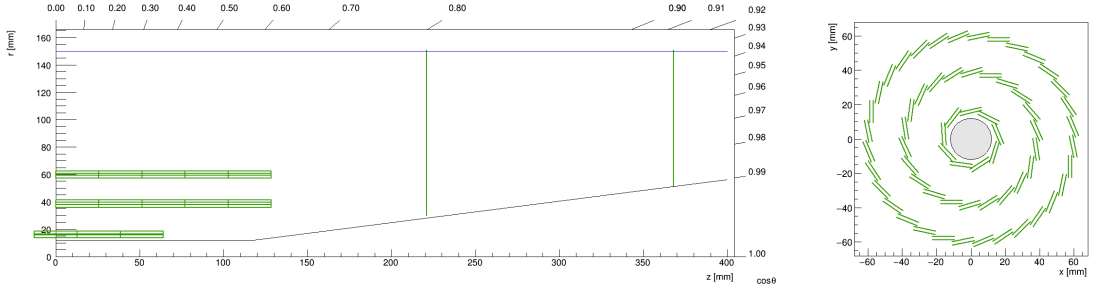

(b) RZ (left) and XY (right) view of vertex layout with beam pipe radius=12mm

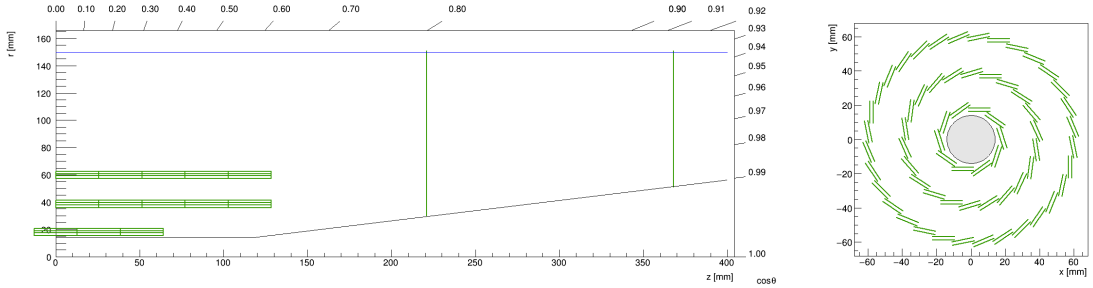

(c) RZ (left) and XY (right) view of vertex layout with beam pipe radius=14mm

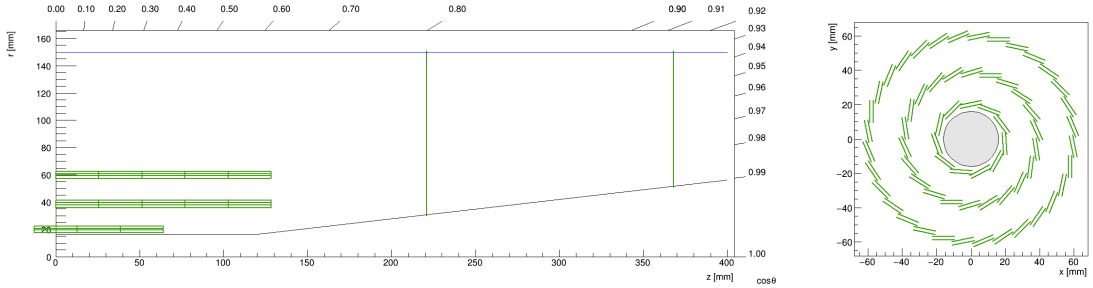

(d) RZ (left) and XY (right) view of vertex layout with beam pipe radius=16mm

Figure 32: RZ view and XY view of vertex layouts with beam pipe radius= 10mm, 12mm, 14mm and 16mm. The black lines in RZ view plots and grey circles in XY view plots show the beam pipe and the blue line outside the vertex barrel is a carbon fiber tube to strengthen the support of the beam pipe.

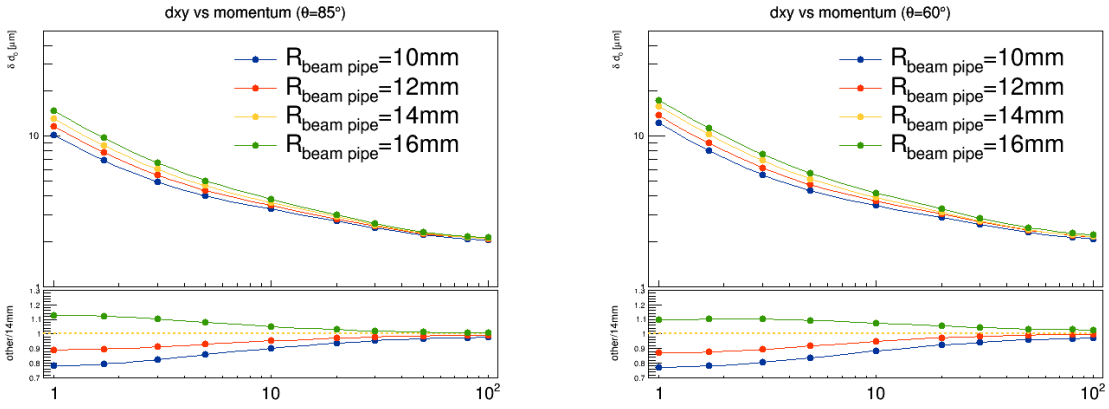

Figure 33: The d0 resolution, as a function of momentum, is compared for different beam pipe radius using single muon tracks at polar angle $\theta = 85°$ and 60°.

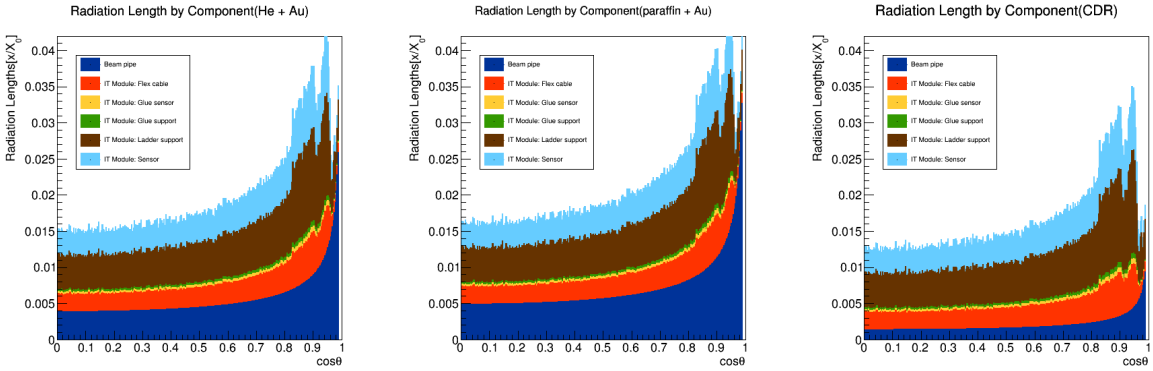

Figure 34: Material budget distribution by components including beam pipe and vertex for different beam pipe design: Helium gas coolant design (left), paraffin coolant design (middle) and CDR design (right). The vertex here is the prototype_v1.

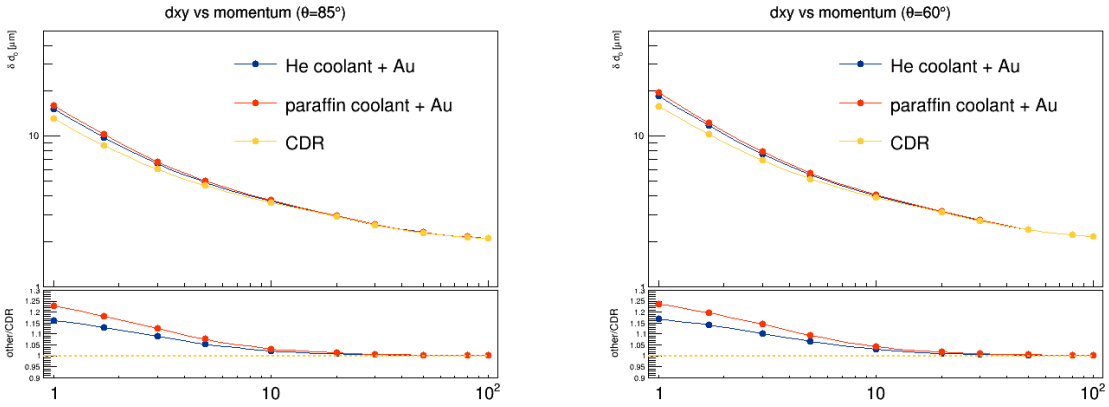

Figure 35: The d0 resolution, as a function of momentum, is compared for optimal layout with different beam pipe design, using single muon tracks at polar angle $\theta = 85°$ and 60°.

	Helium gas coolant	Paraffin coolant	CDR
beam pipe	0.00558	0.00707	0.00203
IT Module: Flex cable	0.00312	0.00312	0.00312
IT Module: Glue sensor	0.00037	0.00037	0.00037
IT Module: Glue support	0.00037	0.00037	0.00037
IT Module: Ladder support	0.00643	0.00643	0.00643
IT Module: Sensor	0.00444	0.00444	0.00444
total	0.02031	0.02180	0.01676

Table 15: Beam pipe and vertex detector material budget of each component for different design: CDR, Helium gas coolant design and paraffin coolant design.

quickly build tracker geometry based on module level and compute all kinds of tracking performance. Because this is the first study using tkLayout for CEPC, hard-code modification and cross-checking will be necessary in the future.

An optimal vertex layout is got, which contains three same length double layer in the barrel and three double disks in the endcap. This optimal vertex layout has better d0 resolution than the CDR vertex and long barrel vertex, but it is still an ideal design due to no air cooling design for disk and no detail mechanical design. Hence the next step is to cooperate with engineer to find whether there are engineering solutions for this optimal vertex layout. Meanwhile, full simulation validation of this optimal vertex layout is necessary.

We investigate some new disk arrangements which will make a hole in the disk providing a path for airflow to cool down the vertex detector. The d0 resolution result of those layouts shows that the effect is very small when we make those rearrangements, but we still need to consider real mechanics and heat dissipation simulation.

The impact of beam pipe radius and beam pipe design on the vertex d0 resolution is also studied. Smaller beam pipe radius can improve vertex d0 resolution but causing higher beam background. Different beam pipe design, causing different beam pipe material budget, has big effect on the vertex d0 resolution especially for low momentum tracks. So the next step is to find lower material coolant and to make Beryllium layer thicker.

References

[1] CEPC Study Group Collaboration, M. Dong et al., arXiv:1811.10545 [hep-ex].

[2] N. Alipour Tehrani and P. Roloff,. https://cds.cern.ch/record/1742993.

Appendices